AB

LAL 01-39
September 2001

Laboratoire de l'Accélérateur Linéaire

Ten years of b-physics at LEP and elsewhere

P. Roudeau

Laboratoire de l'Accélérateur Linéaire,
IN2P3-CNRS et Université de Paris-Sud, BP 34, F-91898 Orsay Cedex

Lectures given at the 29th International Meeting on Fundamental Physics
Sitges (Spain), 5-9 February 2001

U.E.R
de
l'Université Paris-Sud

Institut National
de Physique Nucléaire
et de Physique des Particules

B.P. 34 ~ Bâtiment 200 ~ 91898 ORSAY CEDEX

LAL 01-39
September 2001

Ten years of b-physics at LEP and elsewhere

P. Roudeau

Laboratoire de l'Accélérateur Linéaire
CNRS-IN2P3 et Université de Paris-Sud - Bât. 200 - BP 34 - 91898 Orsay cedex

Abstract

During these lectures I would like to indicate how some measurements and theoretical developments done during the past ten years, before the start-up of b factories, on b-hadron production characteristics and decay properties, have improved our knowledge of the flavour sector of the Standard Model. In most of these measurements, LEP experiments have played an important role.

Lectures given at the 29th International Meeting on Fundamental Physics
Sitges (Spain), 5-9 February 2001

Contents

1 The LEP b-physics program **3**
- 1.1 1989: program definition . . . 3
- 1.2 1990-1995: the learning phase . . . 3
- 1.3 Final results: 1995-2001.... . . . 4

2 b-hadron production characteristics at high energies **4**

3 b-hadron production rates in b-jets **7**

4 The π^* industry **8**

5 b-baryons **10**
- 5.1 First signals: 1990 . . . 10
- 5.2 b-baryons in 2001 . . . 10

6 The $\overline{B_s^0}$ meson **11**
- 6.1 First signals in 1992 . . . 11
- 6.2 The $\overline{B_s^0}$ meson in 2001 . . . 11

7 The Heavy Flavour Steering Group Activities. **12**

8 The inclusive b-hadron lifetime **12**

9 b-hadron lifetimes **13**
- 9.1 b-hadron lifetimes measurements . . . 14
- 9.2 b-hadron lifetimes and theory . . . 14
- 9.3 Predictions on b-meson lifetimes ratios . . . 15
- 9.4 Predictions for b-baryon lifetimes . . . 16

10 Decay width difference in the $B_s^0 - \overline{B_s^0}$ system **16**

11 $B_d^0 - \overline{B_d^0}$ oscillations **19**
- 11.1 Before LEP . . . 20
- 11.2 Δm_d in year 2000 . . . 20

12 Search for $B_s^0 - \overline{B_s^0}$ oscillations **20**

13 Heavy hadrons decay constants **23**
- 13.1 Charm hadron decay constant . . . 23
- 13.2 B meson decay constant . . . 25

14 Charm counting in b-hadron decays **25**
- 14.1 Charmonium production in b-hadron decays . . . 25
- 14.2 Open-charm counting . . . 26
- 14.3 Inclusive charm counting . . . 27
- 14.4 Wrong-sign charm production . . . 28
- 14.5 Global average for charm production . . . 29

15 Inclusive semileptonic branching fraction of b-hadrons 30

16 Measurement of $|V_{cb}|$ in inclusive semileptonic b-hadron decays 30

17 Heavy quark masses 32
17.1 The b-quark mass 32
17.2 Other heavy quark masses 33

18 b-meson exclusive semileptonic decays 33
18.1 $\overline{B^-} \to D^0 \ell^- \overline{\nu_\ell}$ 33
18.2 $\overline{B^0_d} \to D^{*+} \ell^- \overline{\nu_\ell}$ 34

19 $|V_{cb}|$ measurements at LEP 35

20 Excited states in b-hadron semileptonic decays 36

21 Measurements of $|V_{ub}|$ at LEP 38

22 Quark mass matrices 39

23 CKM matrix parametrization 40
23.1 Measurements of the parameters λ and A 40
23.2 Constraints on the two other parameters: ρ and $i\eta$ 41
23.3 Unitarity test before b-factories 41
23.4 Measurements of the CKM triangle parameters before b-factories 42
23.5 Present anomalies or expectations 44
23.6 Evolution of the allowed $(\rho,\ \eta)$ plane region 45

24 Conclusions 47

1 The LEP b-physics program

1.1 1989: program definition

The main lines were defined during a special session of a meeting held in Moriond in March 1989. A similar meeting, with similar conclusions, happened in SLAC at the end of July 1989.

Studies of b-hadrons were made possible because of the developments of silicium vertex detectors which allow to exploit the production characteristics of b-particles emitted in Z boson decays. At that time it was realized that:

- because of the expected statistics, inclusive or semi-inclusive b-hadron decays had to be studied in place of exclusive channels for which very few events were expected.
- semileptonic decays allowed to distinguish between the different types of b-hadrons. As an example, a Λ_c^+ accompanied by a negative lepton, in a jet, signs a b-baryon. For baryons it is not even necessary to reconstruct completely the Λ_c^+ charmed baryon and $p - \ell^-$ or $\Lambda - \ell^-$ correlations are sufficient. Similarly, $D^{*+} - \ell^-$ pairs in a jet, provide events samples enriched in $\overline{B_d^0}$ semileptonic decays. As a result, properties of the different b-hadrons can be studied.
- the Cabibbo, Kobayashi and Maskawa (CKM) matrix element, V_{cb}, which governs the $b \to c$ weak transition could be measured by studying $\overline{B} \to D\ell^-\overline{\nu_\ell}$ decays. After the developments of the Heavy Quark Effective Theory (HQET) it has been realized that theoretical uncertainties will be under better control if semileptonic decays with a D^* in the final state were used.
- jets induced by b and $\bar{b}$ quarks could be distinguished using the sign of an identified lepton emitted at large transverse momentum relative to the jet axis or using the jet charge. This quantity is the weighted average of the jet particles charges. The weight being the value of the particle momentum projected along the jet axis raised to some power κ[1].
- study of $B_d^0 - \overline{B_d^0}$ oscillations was expected to be easy.
- study of $B_s^0 - \overline{B_s^0}$ oscillations was expected to be, on the contrary, very difficult. As the oscillation frequency was anticipated to be high, the decay time of b-hadrons had to be measured. At that time it was difficult to evaluate the possible reach of LEP and SLD collaborations.

1.2 1990-1995: the learning phase

Before the start of b-factories the main contributors to the physics of b-hadrons were using $e^+ - e^-$ colliders operating at the $\Upsilon(4S)$ (ARGUS, CLEO) or at the Z mass (LEP, SLD) and the TeVatron (CDF) which is a $p - \overline{p}$ collider generating collisions at $\sqrt{s} = 1.8$ TeV. Registered statistics and production characteristics of b-hadrons are very different in these three experimental conditions as indicated in Table 1.

[1]Typical values for κ are between 0.5 and 1.

Experiment	# $b-\bar{b}$ events	environment
LEP Collaborations	1 M each	Z decays, back-to-back 45 GeV b-jets
SLD	0.1 M	Z decays, back-to-back 45 GeV b-jets
ARGUS	0.2 M	$\Upsilon(4S)$, B_d^0 and B^+ mesons at rest
CLEO	3-9 M	$\Upsilon(4S)$, B_d^0 and B^+ mesons at rest
CDF	several M	$\sqrt{s} = 1.8$ TeV, triggered events mainly with leptons

Table 1: *Summary of registered statistics and production characteristics of b-hadrons.*

In spite of the small statistics collected by SLD, this experiment provides important contributions in several analyses because of the properties of its pixel detector situated much closer to the beam line than the LEP silicon strip detectors.

This time period was mainly a learning phase during which "new" signals have been isolated and "new" ideas emerge. Among the new phenomena observed at LEP one can mention the evidence for b-baryons (Λ_b^0, Ξ_b), for the $\overline{B_s^0}$ meson, for B^{**} states and for the time dependence of $B_d^0 - \overline{B_d^0}$ oscillations. Among the new ideas let's quote the amplitude method developed by ALEPH to study $B_s^0 - \overline{B_s^0}$ oscillations and the partial reconstruction of the D^{*+} meson developed by DELPHI to study the semileptonic decay channel $\overline{B_d^0} \to D^{*+}\ell^-\overline{\nu_\ell}$.

1.3 Final results: 1995-2001....

LEP stops running at the Z pole in 1995 but it appears that analyses on heavy flavours have not yet been completed.

Some data samples have been reprocessed in 1997-1998 to benefit from improvements obtained in track reconstruction, detector alignment, particle identification, ... algorithms. Algorithms to analyze events get also more complex and powerful, providing a better use of the information. As a result, since 1995, large improvements have been obtained in accuracy and unexpected results have been obtained on difficult channels as the measurement of $|V_{ub}|$ and the limit on the oscillation parameter, Δm_s, of the $B_s^0 - \overline{B_s^0}$ system.

To illustrate what has been learned in b-physics during these years a Tour inside the Standard Model picture of CP violation, before the start of b-factories is proposed.

To quantify the importance of LEP activities in these measurements the LEP weight has been defined as the ratio:

$$LEP_{weight} = \frac{\sigma^2_{All}}{\sigma^2_{LEP}} \qquad (1)$$

between the uncertainty, on a given measurement, provided by all existing results and the uncertainty corresponding to LEP measurements only.

2 b-hadron production characteristics at high energies

At high energy colliders, b-hadrons are emitted during the b-quark fragmentation and, because of the high mass of this quark as compared with Λ_{QCD}, the b-hadron takes a

large fraction of the jet energy. This is illustrated in Figure 1. The average fraction of the LEP beam energy taken by a weakly decaying b-hadron, as measured by ALEPH [1] is:

$$X_E = 0.730 \pm 0.006 \pm 0.006. \quad (2)$$

Similar results have been obtained by OPAL and SLD.

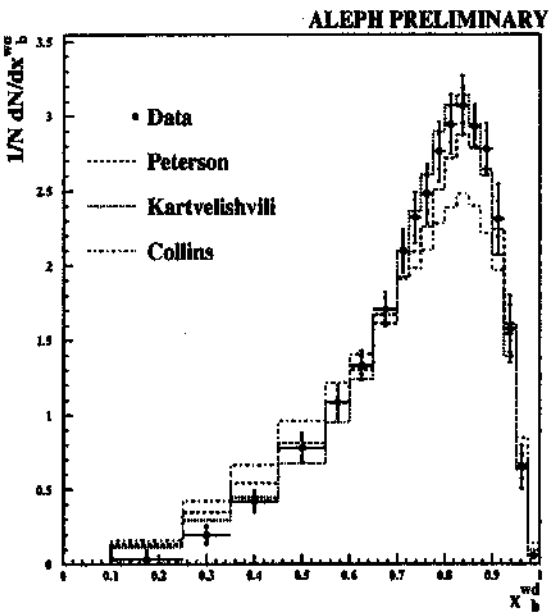

Figure 1: *Reduced energy distribution of the weakly-decaying b-hadron, as reconstructed from data. The smaller error bars are statistical, the wider represent total errors. The best-fit distributions obtained using different models are superimposed.*

Studies of b-hadron properties require the extraction of many informations from registered events:

- the separation between b and non-b events is based on the use of vertex detectors, located as close as possible to the beam interaction point, which are measuring, with a few micron accuracy, the positions of the charged particles trajectories. Because of the lifetime of b-hadrons, of the order of one picosecond, and of their average energy, 33 GeV at the Z pole, the b-hadron decay vertex is situated at a few millimeters from the beam interaction point. Charged particles emitted at these two vertices can thus be separated. The probability that all charged particles originate from the beam interaction point, which is evaluated from the measured particles trajectories, and corresponding uncertainties, is a key ingredient to separate $b - \overline{b}$ events from all other quark flavours produced in hadronic Z decays. Other informations as the presence of identified leptons and the mass of the system of particles attached to a secondary vertex have been also included to enhance the separation between b and non-b events.

- the separation between jets induced by a b, from those induced by a $\overline{b}$ quark, is obtained using several informations. In Z decays, information from the jet opposite to the studied one is obtained by considering the distribution of the jet charge which is centred at negative values in case of b-jets. For a given value of the measured

jet-charge a probability can be evaluated that this jet originates from a b or a $\overline{b}$ quark. As most (80%) of b-hadrons do not oscillate, their decay products contain also information on the initial quark. For instance, negative leptons, leading baryons are signatures for b quarks. In the studied jet, particles originating from the beam interaction point contain also information on the presence of a quark or of an anti-quark at the jet origin.

- to study the time dependence of $B^0 - \overline{B}^0$ oscillations one has to know if a b or a $\overline{b}$ has been produced at $t = 0$ (beam interaction time) and also if a b or a $\overline{b}$ quark is present in the b-hadron at the time of its decay. This last information is obtained from the decay products of the b-hadron. The identification of ℓ^- or of c-hadrons are signatures for b-quark decays, whereas ℓ^+ or $\overline{c}$-hadrons are signatures for a $\overline{b}$.

- the type of the decaying b-hadron can also be identified using reconstructed charmed hadrons emitted in semileptonic decays. Correlations between ℓ^- and D_s^+ or Λ_c^+ are, respectively, signatures for $\overline{B_s^0}$ or Λ_b^0 hadrons. The flavour of leading hadrons produced during the fragmentation of the b quark allows also to select events samples enriched in a given type of b-hadrons. As an example, leading $K^{+/-}$ emitted at the beam interaction point enrich the sample in events with B_s^0 or $\overline{B_s^0}$ mesons.

In Figure 2 are displayed three views of an event registered by ALEPH, which is a candidate for $Z \to b\overline{b}$, b or $\overline{b} \to \overline{B_s^0}$, $\overline{B_s^0} \to D_s^+ \ell^-$ X. The enlarged view, around the beam interaction point, allows to appreciate the separation between charged particles emitted from the main (IP) and from secondary vertices.

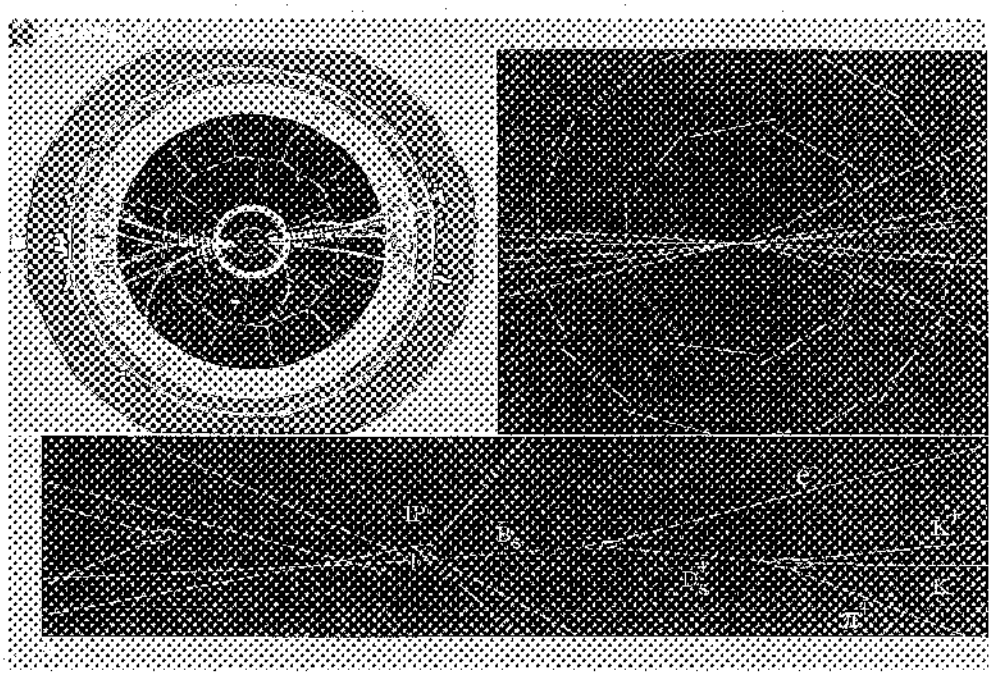

Figure 2: *Display of an event which is a candidate for the following decay chain:* $\overline{B_s^0} \to D_s^+ e^- \overline{\nu}_e$, $D_s^+ \to K^- K^+ \pi^+$.

3 b-hadron production rates in b-jets

To measure the properties of the different types of b-hadrons produced during the hadronisation of a b-quark emitted in high energy collisions it is mandatory to know their production fractions. It appears that their determinations are easier than for c-hadrons produced in c-jets at high energy because of B^* electromagnetic decays and of oscillations of neutral b mesons.

For charmed hadrons, emitted in c-jets, uncertainties on the production fractions for D_s^+ and Λ_c^+ are governed by those attached to the branching fractions of these particles into a given decay final state, namely [2]:

$$BR(D_s^+ \to \phi\pi^+) = (3.6 \pm 0.9)\%, \; BR(\Lambda_c^+ \to pK^-\pi^+) = (5.0 \pm 1.3)\%. \tag{3}$$

For b-hadrons, decay channels of the type: $\overline{\mathrm{B}}_s^0 \to \mathrm{D}_s^+\ell^-\overline{\nu}_\ell X$ or $\Lambda_b^0 \to \Lambda_c^+\ell^-\overline{\nu}_\ell X$ can be used as well but the fractions of $\overline{\mathrm{B}}_s^0$ and Λ_b^0, evaluated in this way, suffer from the same level of uncertainty as in the previous case, for charm, because the same decay final states for D_s^+ and Λ_c^+ are necessarily involved.

Hopefully additional constraints emerge in case of b-hadron production. The $\overline{\mathrm{B}}_s^0$ and B^- production fractions are expected to be equal:

$$f_{B_s} = f_{B^-} \tag{4}$$

This equality is obtained by noting that, during the hadronization process, $(b\bar{d})$ and $(b\bar{u})$ systems are produced with the same rate (Isospin invariance coming from the fact that $m_u \simeq m_d << \Lambda_{QCD}$). Decays of produced resonances can induce asymmetries between the amount of weakly decaying $\overline{\mathrm{B}}_q^0$ and B^- mesons. Such asymmetries are large in case of charm hadrons (mainly due to the fact that $\mathrm{D}^{*0} \not\to \mathrm{D}^+\pi^-$ because of the values of the masses involved). In case of b-hadrons, all B^* states decay electromagnetically and the symmetry is maintained between $\overline{\mathrm{B}}_q^0$ and B^- mesons. Higher excited states are not either expected to generate an asymmetry because their masses are away from thresholds for $\mathrm{B}\pi$ or $\mathrm{B}^*\pi$ production[3].

Another constraint, which applies to the production fractions of neutral b-mesons, originates from oscillations in the $\mathrm{B}_{d,s}^0 - \overline{\mathrm{B}}_{d,s}^0$ systems. The integrated oscillation rate, χ, is the probability that, having produced a B^0, a $\overline{\mathrm{B}}^0$ is observed when it decays. This rate can be measured in $Z \to b\bar{b}$ events from the rate of same-sign dileptons. These are events containing two leptons of same charge, emitted at large transverse momentum (typically more than 1 GeV) relative to the jet axis and situated in the two opposite jets. This rate receives two contributions: from B_d^0 and B_s^0 oscillations. As explained in Section 11, the integrated rate for oscillations of the $\mathrm{B}_d^0 - \overline{\mathrm{B}}_d^0$ system alone, χ_d, has been measured and studies of oscillations of the $\mathrm{B}_s^0 - \overline{\mathrm{B}}_s^0$ system ensure that $\chi_s \simeq 0.5$ with an excellent accuracy. Consequently one has the additional constraint on $\overline{\mathrm{B}}_d^0$ and $\overline{\mathrm{B}}_s^0$ production fractions:

$$\bar{\chi} = f_{B_s}\chi_d + f_{B_d}\chi_s. \tag{5}$$

Experimentally it has also been possible to separate charged particles emitted at the beam interaction point from those emitted at the b-hadron decay vertex, using their

[3] More details on production characteristics of B^* and B^{**} mesons can be found in [3].

measured impact parameters relative to these two positions. b-decay products have also, usually, a higher rapidity than fragmentation particles accompanying the heavy hadron. Using, in addition, the particle charges, these informations can be combined in a single quantity which measures the charge of the weakly decaying b-hadron. In this way a clear separation is obtained between neutral and charged states as shown in Figure 3 [4].

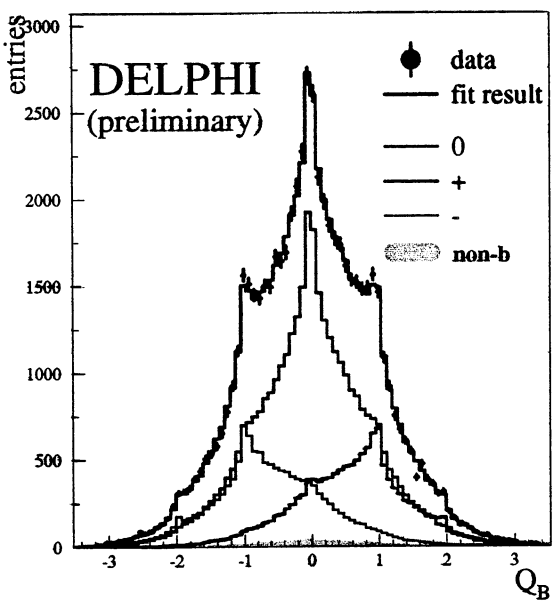

Figure 3: *The vertex charge Q_B for the data (points with error bars) with the result of the fit superimposed (solid histograms). The shapes for neutral, negatively and positively charged b-hadrons obtained from the simulation and used in the fit are also shown. The contribution of non-$b\bar{b}$ events is given as shaded histogram.*

Correcting for an expected small contribution from charged-strange b-baryon decays, they obtain:

$$f_{\mathrm{B}^+} = (41.4 \pm 1.6)\%. \tag{6}$$

All informations on b-hadron production rates produced by LEP experiments and CDF have been combined, and the constraints expressed by Equations (4) and (5) have been imposed giving:

$$f_{\mathrm{B}^+} = f_{\mathrm{B_d}} = (40.0 \pm 1.0)\%, \tag{7}$$

$$f_{\mathrm{B_s}} = (9.7 \pm 1.2)\%, \tag{8}$$

$$f_{b\text{-baryon}} = (10.4 \pm 1.7)\%. \tag{9}$$

More detailed informations and updated results can be found in: http://lepbosc.web.cern.ch/LEPBOSC/.

4 The π^* industry

This idea was developed by DELPHI [5] to study the semileptonic decay $\overline{\mathrm{B}^0_d} \to \mathrm{D}^{*+}\ell^-\overline{\nu_\ell}$. Having isolated a candidate lepton track, an algorithm defines a bunch of tracks (charged and neutrals), which are candidates as decay products of the charmed hadron. Candidates

for the charged pion (π^*), coming from the D^{*+} cascade decay, are then considered by using all charged hadrons in the jet and taking separately those having the same or an opposite charge as the lepton. If the candidate is among the particles retained as D decay products one computes the mass difference $\Delta(M) = M_{N_D} - M_{N_D-1}$ in which N_D is the number of D decay products candidates and $N_D - 1$ corresponds to this system once the candidate π^* has been removed. If the candidate is among other charged tracks produced in the jet, one computes the difference: $\Delta(M) = M_{N_D+1} - M_{N_D}$, where N_D+1 corresponds to the system of D decay products augmented with the candidate π^*. In case of real D^{*+} decays, there is an excess of events at low values of $\Delta(M)$ when the lepton and the π^* have opposite charges. It has been verified that wrong sign combinations provide an accurate description of the combinatorial background. Signal events include a contamination from $B^- \to D^{*+}\ell^-\overline{\nu_\ell}X$ decays which has to be subtracted using simulated events from this decay channel.

In this approach, large samples of $\overline{B_d^0} \to D^{*+}\ell^-\overline{\nu_\ell}$ semileptonic decays can be accessed as compared with analyses in which the D^0 is completely reconstructed. In the latter, the combinatorial background under the D^{*+} $\Delta(M)$ peak is much reduced but the former appears to have the best sensitivity. This approach has been used also to measure the $\overline{B_d^0}$ meson lifetime (DELPHI [6]), to study $B_s^0 - \overline{B_s^0}$ oscillations (DELPHI [7], OPAL [8]) and to extract $|V_{cb}|$ (DELPHI [9], OPAL [10]). An example of $\Delta(M)$ mass distributions, as obtained by OPAL, are displayed in Figure 4.

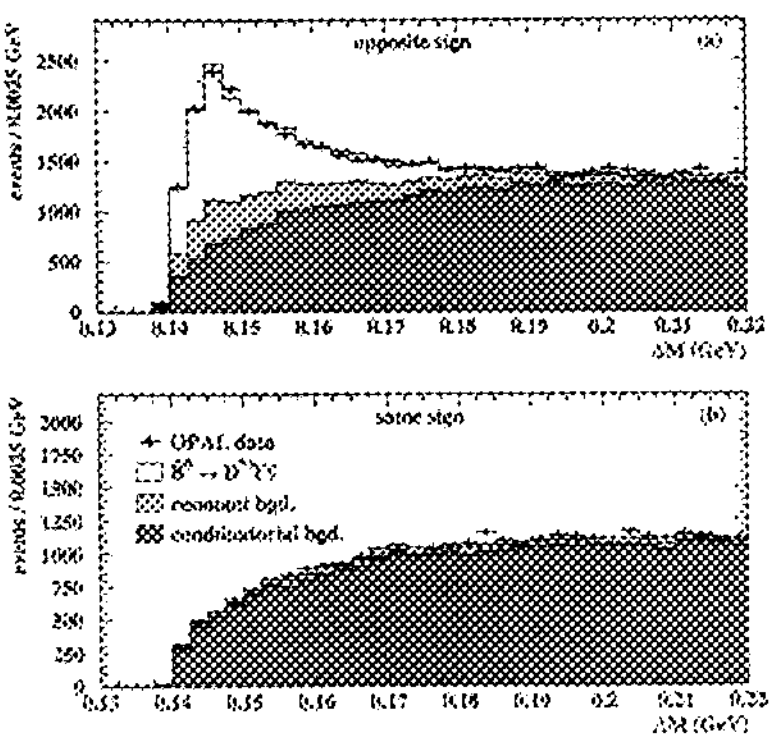

Figure 4: Reconstructed $\Delta(M)$ distributions for selected (a)opposite sign and (b) same sign lepton-pion combinations.

5 b-baryons

5.1 First signals: 1990

The first signals from b-baryons were observed by ALEPH in 1990 [11]. In Figure 5-left, the excess of Λ hyperons accompanied by a negative lepton as compared with those accompanied by a positive lepton is visible. This behaviour was expected for events containing, in a jet, a b-baryon decaying semileptonically.

Using a similar approach, but correlating Ξ^- hyperons with leptons and developing special algorithms to reconstruct the trajectory of the Ξ^- within the silicon vertex detector, DELPHI finds evidence for weakly decaying strange b-baryons, Ξ_b, in 1995 [12].

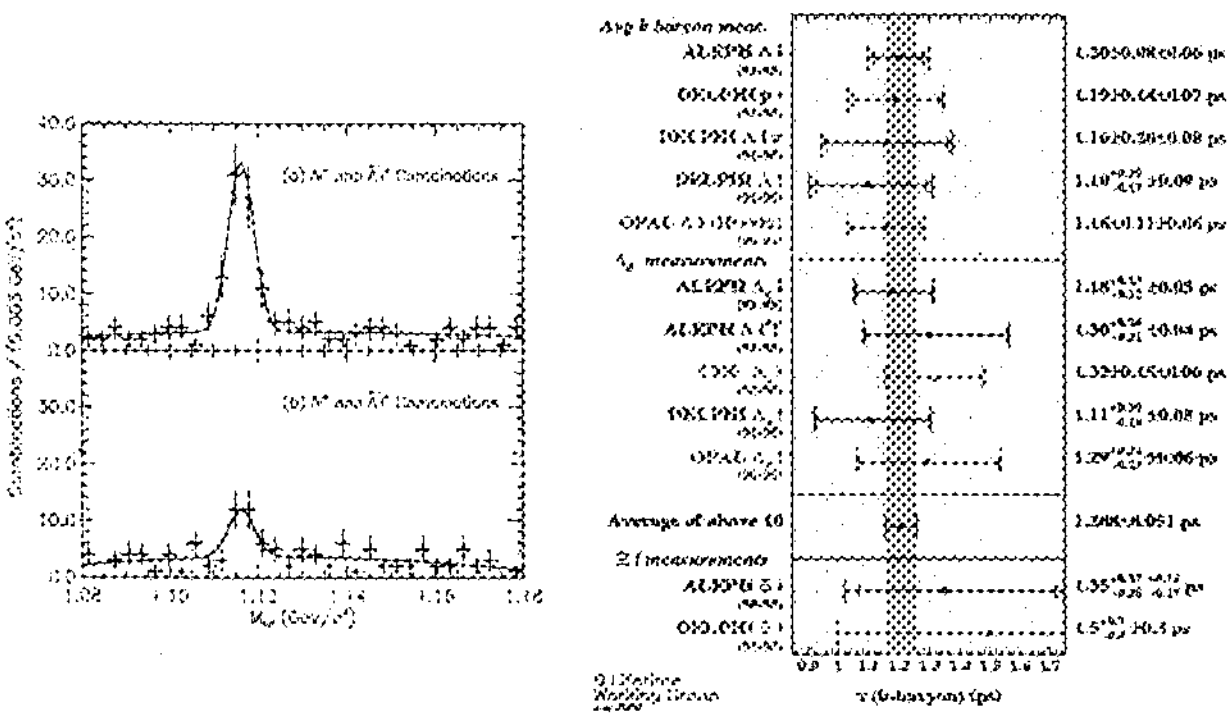

Figure 5: *Left: Λ signals associated to right (a) and wrong (b) sign leptons, registered by ALEPH. Right: b-baryon lifetime measurements. The darker area corresponds to the present average of the measurements given in the figure. Internal error bars correspond to statistical uncertainties and full error bars include systematics.*

5.2 b-baryons in 2001

Other types of correlations between baryons and leptons have been studied as $p-\ell$ and $\Lambda_c^+-\ell$. Correlations between baryons and anti-baryons, emitted from the beam interaction point and from the b-hadron decay vertex, have also been considered.

This allows to isolate events samples enriched in b-baryons from which several results have been obtained. The b-baryon production rate (see Section 3) is known with an uncertainty of 16% which is noticeably better than the relative uncertainty, of 26%, on the Λ_c^+ absolute branching fractions. By considering the energy distributions of charged

lepton and neutrino in b-baryons semileptonic decays, the polarization of Λ_b^0 baryons produced at LEP has been measured [13]:

$$\mathcal{P}(\Lambda_b^0) = -0.45^{+0.39}_{-0.17} \tag{10}$$

This value indicates that the initial polarization of b-quarks, emitted from Z decays, which amounts to $\mathcal{P}(b) = -0.94$, is not entirely transmitted to the Λ_b^0. This result can be explained by considering the intermediate creation of excited b-baryons as $\Sigma_b^{(*)}$ states which induce depolarization effects [14].

Several measurements of the b-baryon lifetime have been obtained by LEP and CDF experiments. They are summarized in Figure 5-right. Average values for b-hadron lifetimes are obtained by the LEP lifetime working group: http://claires.home.cern.ch/claires/leplife.html. It results that the b-baryon lifetime is 30% lower than the average lifetime of b-mesons; this difference has not yet received a satisfactory explanation from theory (see Section 9.4).

The value of the Λ_b^0 mass has been measured mainly by CDF as it needs the reconstruction of exclusive final states. The sensitivity of TeVatron experiments, using triggers on $J/\psi \to \mu^+\mu^-$ decays, is much higher as compared with the sensitivity of LEP experiments for such channels.

6 The $\overline{B}_s^0$ meson

6.1 First signals in 1993

Before LEP, there were indirect signals of $\overline{B}_s^0$ meson production. The rate of same sign dilepton events measured by UA1 [31], in 1987, was expected to receive contributions from B_d^0 and B_s^0 oscillations. In 1990, when running at the $\Upsilon(5S)$, the CUSB collaboration [15] measured the broadening of cascade decay, $B^* \to B\gamma$, photon rays due to the movement of B^* mesons (Doppler effect). As B_d^* and B_s^* mesons have different moments, the measured photon energy distribution gives evidence for B_s^0 production.

More direct signals corresponding to the semileptonic decay: $\overline{B}_s^0 \to D_s^+ \ell^- \bar{\nu}_\ell X$ have been identified by DELPHI in 1992 [16]. In Figure 6-left is given a copy of the first page of the DELPHI bulletin issued at that time.

6.2 The $\overline{B}_s^0$ meson in 2001

The $\overline{B}_s^0$ meson is still studied using mainly the $D_s^- \ell^+$ final state. Its production fraction in b jets is known with 12% accuracy in spite of the fact that the uncertainty on absolute branching fractions of the D_s^+ meson is 25%. This has been explained in Section 3. Several measurements exist of the $\overline{B}_s^0$ lifetime which are summarized in Figure 6-right. A possible difference between the decay widths of the mass eigenstates of the $B_s^0 - \overline{B}_s^0$ system has been searched for. In this respect, lifetime measurements for pure $\overline{B}_s^0$ states, corresponding to $D_s^+ \ell^-$ semileptonic decays, and for enriched samples in CP even final states as $\overline{B}_s^0 \to \phi\phi X$ candidates have been compared. The present limit:

$$\Delta\Gamma(B_s^0)/\Gamma(B_s^0) < 0.31 \text{ at } 95\% \text{ C.L.} \tag{11}$$

is still far away from current theoretical expectations for this ratio which are of the order of 5-10% (see Section 10).

The accuracy on the measurement of the $\overline{B_s^0}$ mass is dominated by CDF for the same reasons, explained in case of the Λ_b^0 mass measurement (section 5.2).

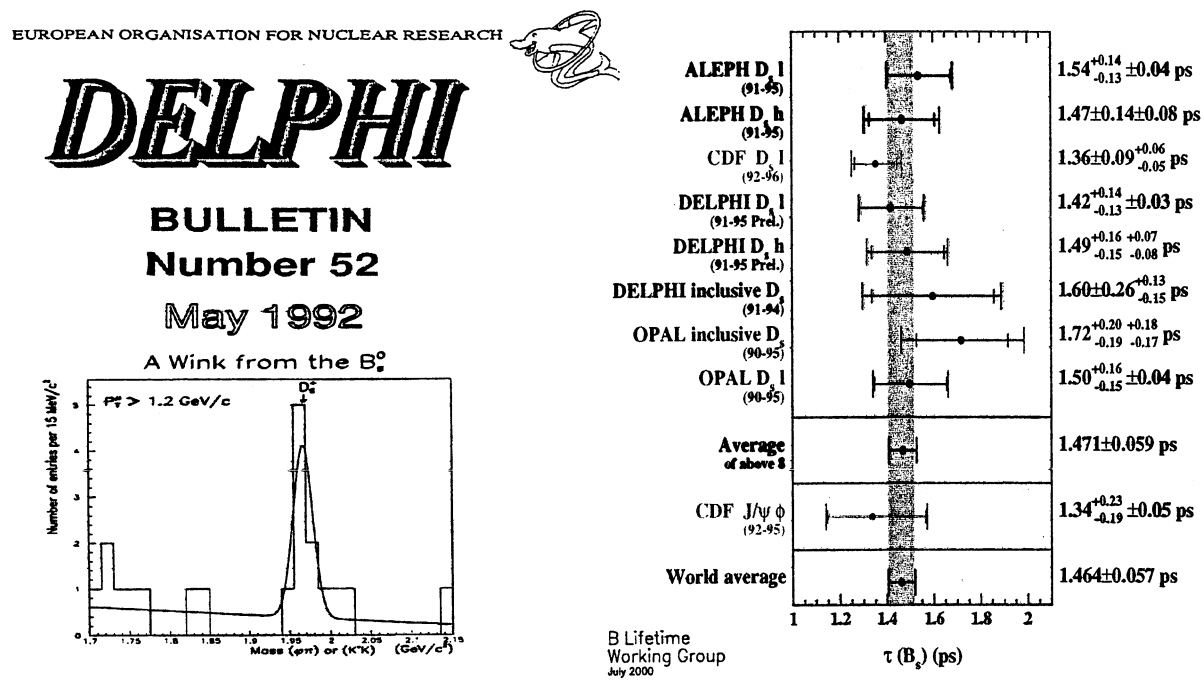

Figure 6: *Left: copy of the front page of the DELPHI bulletin when first $\overline{B_s^0}$ signals appear. Right: $\overline{B_s^0}$ lifetime measurements (same conventions as in Figure 5).*

7 The Heavy Flavour Steering Group Activities.

Since several years working groups have been created to obtain averaged values for important quantities in b-physics as b-hadron lifetimes and production fractions, oscillations of $B_d^0 - \overline{B_d^0}$ and $B_s^0 - \overline{B_s^0}$ systems, decay width differences between mass eigenstates of the $B_s^0 - \overline{B_s^0}$ system and values for the CKM matrix elements $|V_{cb}|$ and $|V_{ub}|$. Activities of these groups are coordinated by a steering group having representatives from ALEPH, CDF, DELPHI, L3, OPAL and SLD collaborations. The corresponding WWW page address is: http://lephfs.web.cern.ch/LEPHFS/ from which pages for the different groups can be accessed. Reports, summarizing results made available by the collaborations in Summer 1999 and 2000 have been prepared [13]. A final publication is expected in 2002.

8 The inclusive b-hadron lifetime

The inclusive b-hadron lifetime is the weighted average of the different b-hadron lifetimes with weights corresponding to their respective production fractions:

$$\tau_b = f_{B_d}\tau(B_d^0) + f_{B^+}\tau(B^+) + f_{B_s}\tau(B_s^0) + f_{b\text{-baryon}}\tau(b-\text{baryon}). \qquad (12)$$

In Figure 7-left, is given the time evolution of the averaged b-hadron lifetime. Before the start of LEP1, it was close to 1.2 ps and even the first LEP results were not much different. Finally it went up and reached stability in 1994. Reasons for this evolution have not been really understood.

In Figure 7-right, the values of the average b-lifetime obtained using two different events samples have been compared. In one sample, events with an identified lepton are used whereas the other corresponds to general inclusive decays. These two samples may correspond to a different composition in various b-hadron types. As explained in Section 15 the semileptonic widths of all b-hadrons are considered to be equal and thus their respective semileptonic branching fractions are proportional to their lifetimes. It can be shown that, within this hypothesis, the lifetimes obtained using the two samples can be related:

$$\frac{\tau_b^{sl}}{\tau_b} = \frac{\sum_i f_{B_i} \tau(B_i)^2}{\sum_i f_{B_i} \tau(B_i)} = 1.006 \pm 0.003. \quad (13)$$

The numerical value, in the last equality, is obtained using measured production fractions and lifetimes of the different types of b-hadrons. Including this correction, the average b-hadron lifetime is:

$$\tau_b = (1.561 \pm 0.014) \text{ ps}$$

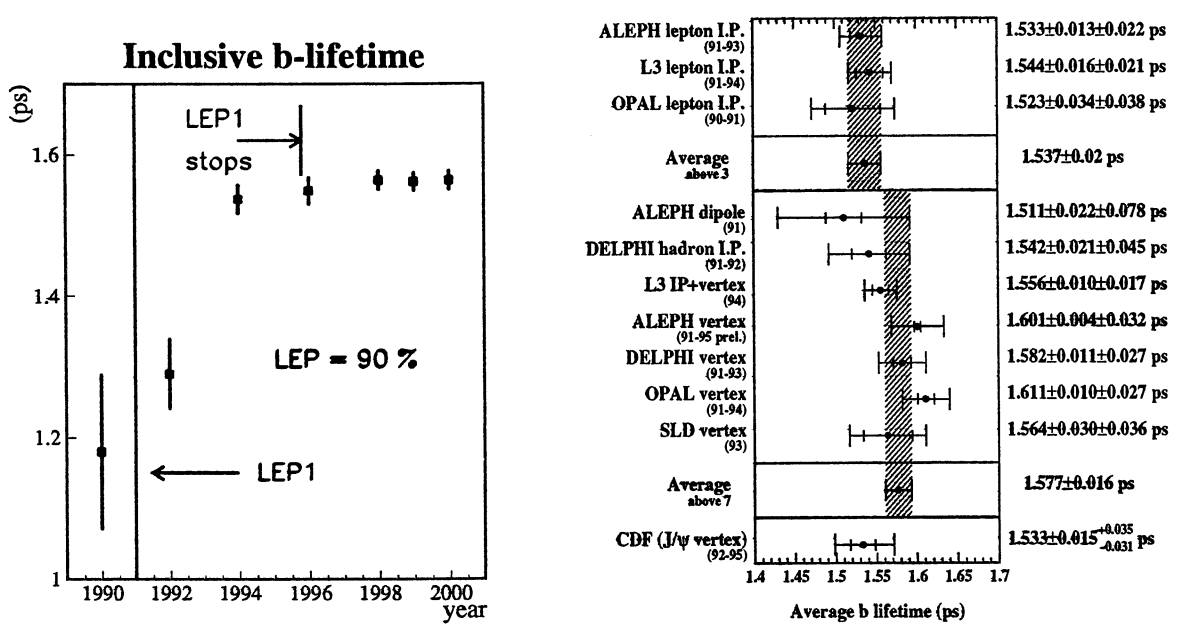

Figure 7: *Left: Evolution in time of the measured inclusive b-hadron lifetime. Right: Present measurements contributing to the average value of the b-hadron lifetime.*

9 b-hadron lifetimes

Individual lifetimes measurements are mandatory inputs to compare measured quantities with theory. This is because, usually, experiments are measuring branching fractions

whereas theorists predict corresponding partial widths. Lifetime measurements give access to the total decay widths of b-hadrons and thus to partial decay widths:

$$\Gamma(\mathrm{B}_i \to \mathrm{X}_j) \;=\; \mathrm{BR}(\mathrm{B}_i \to \mathrm{X}_j) \times \frac{1}{\tau(\mathrm{B}_i)}. \tag{14}$$

9.1 b-hadron lifetimes measurements

As shown in Figure 8, first results on lifetimes for the different types of b-hadrons appear in the 1994 issue of PDG. In spite of the stop of the LEP1 program, at the end of 1995, the accuracy of the measurements has improved enormously since that date. Results are finalized for B_s^0 and b-baryon lifetimes, since 1999, but large improvements have been obtained on the measurements of B_d^0 and B^+ lifetimes, even in 2000 and several analyses are still ongoing.

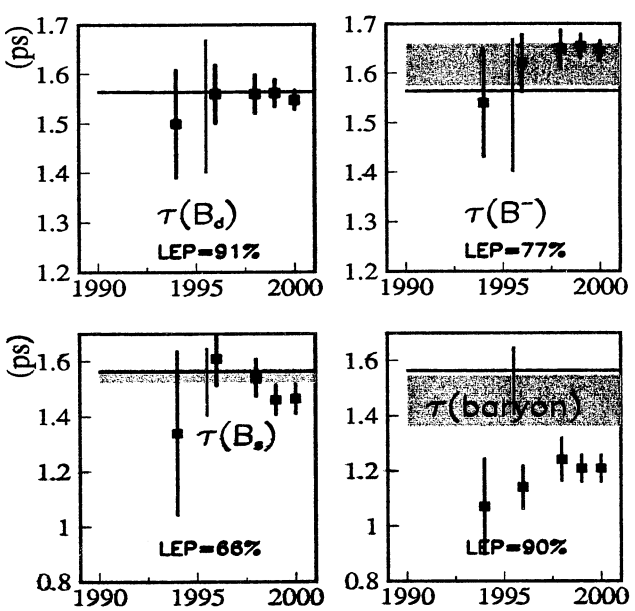

Figure 8: *Evolution with time of the measured b-hadron lifetimes. The contribution of LEP (by end 2000) in these measurements is given (see Equation (1)).*

9.2 b-hadron lifetimes and theory

Inclusive b-hadron decays, nonleptonic or semileptonic, are usually described using the formalism of Operator Product Expansion. Decay rates are expressed as a sum of operators of increasing dimension and developed in a series with terms of order $\mathcal{O}(\Lambda_{QCD}/m_b)^n$. It has been shown [17] that, in this formalism, there is no correction of order $\mathcal{O}(\Lambda_{QCD}/m_b)$. Another way to express this result is to consider that the decay rate of heavy hadrons is governed by the mass (running) of the heavy quark and not by the mass of the heavy hadron itself. In the latter case, writing $m_{H_b} = m_b + \delta_m$, corrections of order $\mathcal{O}(\Lambda_{QCD}/m_{H_b})^n$

introduce directly $\mathcal{O}(1/m_b)$ terms. A b-hadron decay width into the channel X can be expressed as [18]:

$$\Gamma(H_b \to X) = \frac{G_F^2 m_b^5}{192\pi^3}\left[c_3\left(1 - \frac{\mu_\pi^2(H_b) - \mu_G^2(H_b)}{2\ m_b^2}\right) + c_5\left(\frac{2\mu_G^2(H_b)}{m_b^2}\right) + \mathcal{O}(1/m_b^3)\right]$$

The c_n coefficients can be computed in QCD at some scale and at a given order.

Lifetime differences between b-mesons and b-baryons correspond to $\mathcal{O}(1/m_b^2)$ terms. Other differences as Pauli interference of quarks of identical flavours emitted in the final state or weak scattering and weak annihilation mechanisms correspond to $\mathcal{O}(1/m_b^3)$ terms but they can have non-negligible effects as they are multiplied by a numerical factor which is of the order of $16\times\pi^2$. This is because, whereas the dominant charged weak decay of the b-quark gives rise to three partons in the final state, the latter two mechanisms involve only two partons.

9.3 Predictions on b-meson lifetimes ratios

Theoretical predictions [18] and present measurements are given below:

$$\begin{array}{lll} \frac{\tau(\mathrm{B}^+)}{\tau(\mathrm{B}_d^0)} = 1. + \mathcal{O}(1/m_b^3) & = 1 + 0.05 \times \frac{f_B^2}{(200\ MeV)^2} & \leftrightarrow 1.066 \pm 0.020\ (exp.) \\ \frac{\tau(\mathrm{B}_s^0)}{\tau(\mathrm{B}_d^0)} = 1. + \mathcal{O}(1/m_b^3) & = 1 + \mathcal{O}(1\ \%) & \leftrightarrow 0.946 \pm 0.039\ (exp.) \end{array}$$

These predictions for the lifetimes ratios are from 1992, using the vacuum insertion approximation to evaluate the contributions from non-perturbative matrix elements. The ratio between the B^+ and B_d^0 lifetimes can be written [19]:

$$\frac{\tau(\mathrm{B}^+)}{\tau(\mathrm{B}_d^0)} = 1 + k_1 B_1 + k_2 B_2 + k_3\epsilon_3 + k_4\epsilon_4 \qquad (15)$$

In this expression the coefficients k_i can be evaluated from perturbative QCD at some scale μ whereas the other coefficients correspond to averaged values of non-perturbative quantities. In the vacuum insertion approximation, used in [18]: $B_1 = B_2 = 1$ and $\epsilon_3 = \epsilon_4 = 0$. The initial prediction from [18] was criticized, in 1996 [19], after having noted that the (calculable) coefficients k_1 and k_2 are close to zero whereas k_3 and k_4 are close to unity. As a consequence, a small deviation of ϵ_i from zero can give large effects and the authors concluded that the value of the ratio between B^+ and B_d^0 lifetimes was in fact not predictible within $\pm 15\%$. But, in 1998 a lattice QCD evaluation [20] of the matrix elements confirms the initial prediction:

$$B_1 = 0.98(8),\ B_2 = 0.93(5),\ \epsilon_3 = 0.01(3),\ \epsilon_4 = 0.00(2) \qquad (16)$$

giving:

$$\frac{\tau(\mathrm{B}^+)}{\tau(\mathrm{B}_d^0)} = 1.04 \pm 0.02 \pm (0.01 - 0.03) \qquad (17)$$

where the last quoted uncertainty corresponds to the variation on the renormalisation scale. This is a remarkable achievement for the theory and also a nice performance for the experiments which did this measurement with 2% accuracy.

The predicted ratio between the B_d^0 and B_s^0 lifetimes is expected to be unity within $\pm 1\%$ and this estimate appears to be quite general for model builders. A significant measurement in which this ratio differs from 1 will have major consequences on the theory. Unfortunately statistics registered at CDF, LEP and SLD do not allow, at present, to reach accuracies better than 4%. It is thus necessary to await for the TeVatron.

The measurement of the lifetime of the B_c^+ will also constitute an important test for the theory. There are three main contributions to the B_c^+ lifetime coming respectively from the decays of the b- and c-quarks and from the weak-annihilation mechanism. The decay width is expected to be dominated by the c-quark decays and, including $\mathcal{O}(1/m_c^2)$ corrections: $\tau(B_c^+) \simeq \tau(D^0)$ [18]. There also, the TeVatron will give the answer.

9.4 Predictions for b-baryon lifetimes

Using the same formalism, predictions for b-baryon lifetimes have not reached the same accuracy as for b-mesons because quark models have to be used to evaluate non-perturbative matrix elements involving baryons. The present estimate for the Λ_b^0 lifetime is:

$$\frac{\tau(b-baryon)}{\tau(B_d^0)} = 0.98 + \mathcal{O}(1/m_b^3) = 0.9 - 1.0 \leftrightarrow 0.780 \pm 0.035 \ (exp.) \qquad (18)$$

This prediction is off by about three standard deviations. First results from lattice QCD [21] indicate that $\mathcal{O}(1/m_b^3)$ are quite significant and that the ratio $\frac{\tau(b-baryon)}{\tau(B_d^0)} =$ 0.91(1), 0.93(1). The remaining part of the discrepancy (50%) has to be identified. Several possibilities exist; it can come from higher order terms, improved lattice calculations may fill the gap, it can be due also to parton-hadron duality violation and eventually to an experimental bias.

Within the same theoretical formalism of O.P.E., it exists predictions [18] for other b-baryon lifetimes as:

$$\tau_{\Xi_b^-} > \tau_{\Lambda_b^0} > \tau_{\Xi_b^0}; \quad \frac{\tau_{\Xi_b^-} - \tau_{\Lambda_b^0}}{\tau_{\Lambda_b^0}} = 0.17 \pm 0.04 \qquad (19)$$

All these results have to await for the TeVatron to be tested because exclusive final states of b-baryons have to be reconstructed and large statistics need to be registred.

10 Decay width difference in the $B_s^0 - \overline{B_s^0}$ system

In weakly decaying neutral $P^0 - \overline{P}^0$ systems, differences between the decay width of the mass-eigenstates originate from decay final states which are common to P^0 and to $\overline{P}^0$. Consequently a decay width difference gives contribution to the oscillation between P^0 and $\overline{P}^0$ mesons. For B_s^0 mesons this mechanism can be illustrated in the following way:

$$\overline{B_s^0}(b\overline{s}) \rightarrow c(\overline{c}s)\overline{s} \leftrightarrow \overline{c}(c\overline{s})s \leftarrow B_s^0(\overline{b}s) \qquad (20)$$

The decay channels in common ($J/\psi\phi$, $D_s^{(*)}\overline{D}_s^{(*)}X$,..) are expected to be CP even in a dominant way. Thus the CP-even state should have the greater decay rate and hence the shorter lifetime. Equation (20) illustrates the important role played by the $W^- \rightarrow \overline{c}s$

coupling and indicates that decay widths differences are expected to be much smaller in the $B^0_d - \overline{B^0_d}$ system (by a factor of the order of $\sin^2\theta_c$ as they correspond to $W^- \to \bar{c}d$ transitions).

Theoretical calculations of the ratio $\Delta\Gamma(B^0_s)/\Gamma(B^0_s)$ at next-to-leading order in QCD give values between 2% and 12% [22, 23]. Dominant uncertainties come from the determination of the B^0_s decay constant, from the scale dependence of perturbative QCD corrections and from non-perturbative corrections of order $1/m_b$.

Searches for possible differences between lifetimes in the $B^0_s - \overline{B^0_s}$ system consist in selecting decay final states having different compositions in CP-even and CP-odd components (it has been assumed that mass and CP eigenstates are identical).

As an example, for semileptonic B^0_s meson decays, the lifetime distribution is the sum of the lifetime distributions for the two mass eigenstates:

$$P_{semi}(t) = \frac{\Gamma^{\rm short}_{B^0_s}\,\Gamma^{\rm long}_{B^0_s}}{(\Gamma^{\rm short}_{B^0_s} + \Gamma^{\rm long}_{B^0_s})}\left[\exp\left(-\Gamma^{\rm short}_{B^0_s}t\right) + \exp\left(-\Gamma^{\rm long}_{B^0_s}t\right)\right]. \qquad (21)$$

When this distribution is fitted using a single exponential, the difference between the fitted and the B^0_s lifetime corresponding to the average of the total decay widths of the two states ($\Gamma(B^0_s) = \frac{1}{2}(\Gamma^{\rm short}_{B^0_s} + \Gamma^{\rm long}_{B^0_s})$) is of second order in $\Delta\Gamma(B^0_s)/\Gamma(B^0_s)$. ALEPH events with two ϕ mesons in the final state or $J/\psi\phi$ decays measured by CDF are expected to be dominated by the CP even channel and are thus more sensitive to a difference in decay partial widths.

Experimental limits on $\Delta\Gamma(B^0_s)/\Gamma(B^0_s)$ have been obtained by fitting decay time distributions of events samples enriched in B^0_s decays and using a parametrization, for signal events, in terms of $\tau(B^0_s)$ and $\Delta\Gamma(B^0_s)/\Gamma(B^0_s)$. The measurements used in this analysis are given in Table 2. Limits on $\Delta\Gamma(B^0_s)/\Gamma(B^0_s)$ have been obtained with or without imposing that the B^0_s and B^0_d lifetimes are equal (see Section 9.3). In the former case the limit at 95% C.L. is equal to: $\Delta\Gamma(B^0_s)/\Gamma(B^0_s) < 0.31$. The present sensitivity is thus far away from the expected theoretical range and we have again to await for measurements at the TeVatron.

Experiment	Selection	Measurement	$\Delta\Gamma(B^0_s)/\Gamma(B^0_s)$
L3 [24]	inclusive b-sample		< 0.67
DELPHI [25]	$\overline{B^0_s} \to D^+_s \ell^- \overline{\nu_\ell} X$	$\tau_{B^{\rm semi.}_s} = (1.42^{+0.14}_{-0.13} \pm 0.03)$ ps	< 0.46
OTHERS [26]	$\overline{B^0_s} \to D^+_s \ell^- \overline{\nu_\ell} X$	$\tau_{B^{\rm semi.}_s} = (1.46 \pm 0.07)$ ps	< 0.30
ALEPH [27]	$B^0_s \to \phi\phi X$	$BR(B^{\rm short}_s \to D^{(*)+}_s D^{(*)-}_s) = (23 \pm 10^{+19}_{-9})\%$	$0.26^{+0.30}_{-0.15}$
ALEPH [27]	$B^0_s \to \phi\phi X$	$\tau_{B^{\rm short}_s} = (1.27 \pm 0.33 \pm 0.07)$ ps	$0.45^{+0.80}_{-0.49}$
DELPHI [25]	$\overline{B^0_s} \to D^+_s$ hadron	$\tau_{B^{D_s-{\rm had.}}_s} = (1.53^{+0.16}_{-0.15} \pm 0.07)$ ps	< 0.69
CDF [28]	$B^0_s \to J/\psi\phi$	$\tau_{B^{J/\psi\phi}_s} = (1.34^{+0.23}_{-0.19} \pm 0.05)$ ps	$0.33^{+0.45}_{-0.42}$

Table 2: *Experimental constraints on $\Delta\Gamma(B^0_s)/\Gamma(B^0_s)$. The upper limits, which have been obtained by the working group (http://lepbosc.web.cern.ch/LEPBOSC/deltagamma_s/), are quoted at the 95% C.L.*

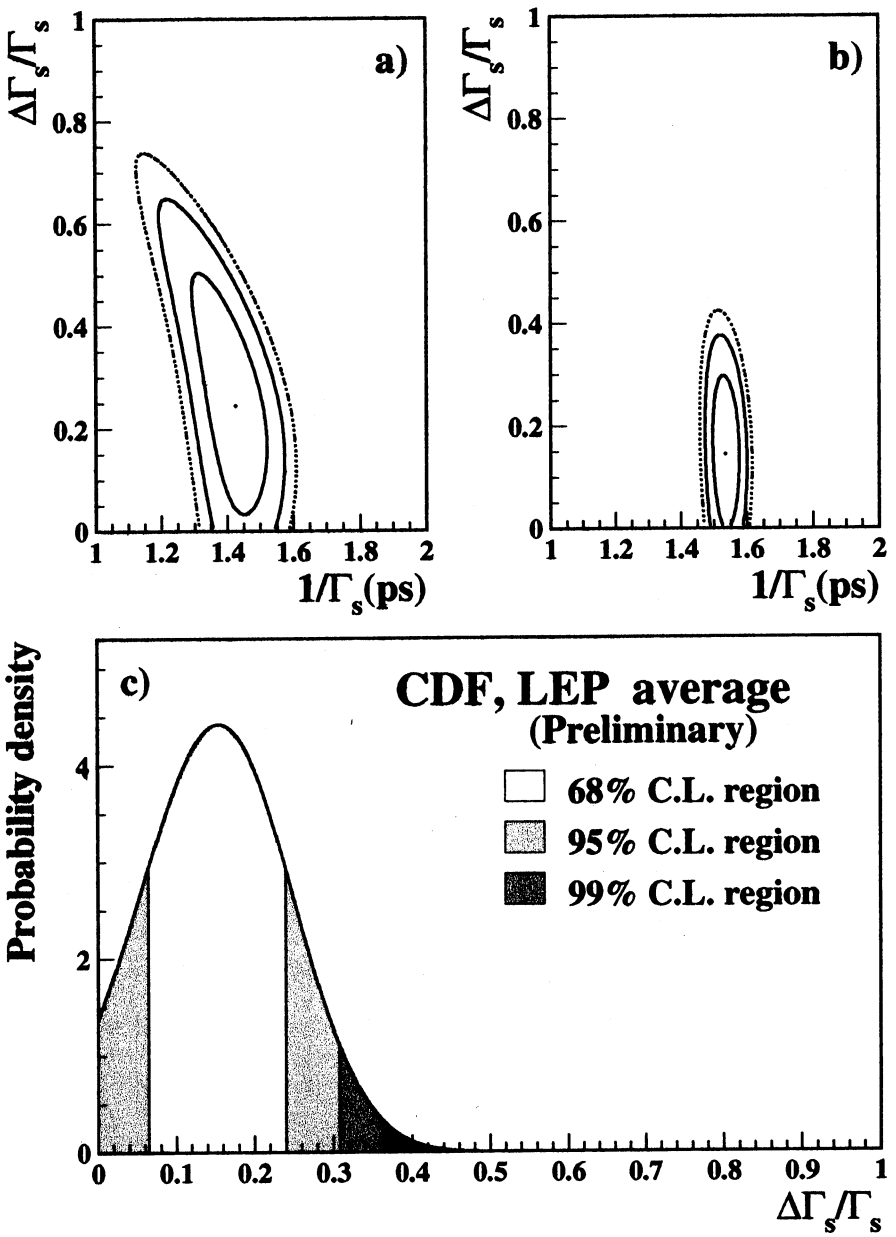

Figure 9: *a) 68%, 95% and 99% C.L. contours of the negative log-likelihood distribution in the plane* $1/\Gamma(B_s^0)$-$\Delta\Gamma(B_s^0)/\Gamma(B_s^0)$. *b) Same as a) but with the constraint* $1/\Gamma(B_s^0) \equiv \tau(B_d^0)$ *supposed to be exact. c) Probability density distribution for* $\Delta\Gamma(B_s^0)/\Gamma(B_s^0)$ *after applying the constraint; the three shaded regions show the limits at the 68%, 95% and 99% C.L. respectively.*

11 $B^0_d - \overline{B^0_d}$ oscillations

The other mechanism which contributes to $B^0 - \overline{B}^0$ oscillations is through virtual states which are common to the two mesons. They correspond to box diagrams, one example being illustrated in Figure 10.

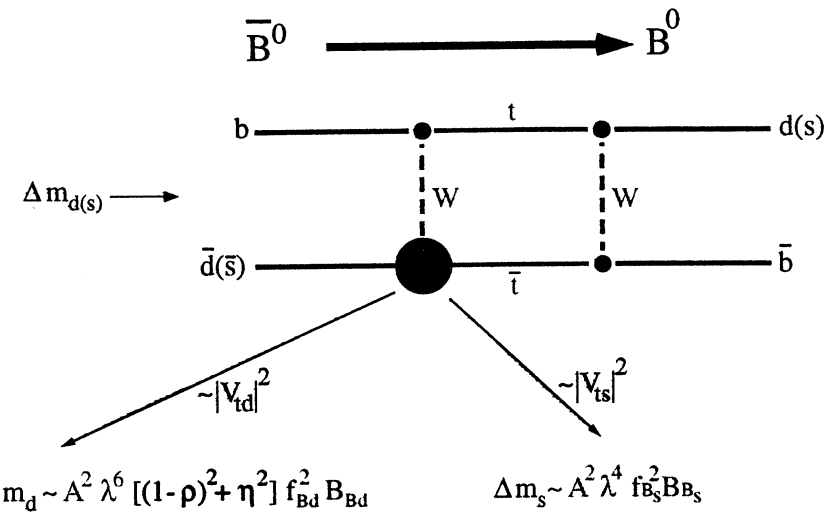

Figure 10: *Example of a box-diagram contributing to the mass difference between mass eigenstates of the* $B^0 - \overline{B}^0$ *system.*

For B mesons this is the dominant process, oscillations corresponding to decay width differences (see Section 10) can be neglected. This is because, at first order, the decay widths and mass differences between the mass eigenstates are related [29]:

$$\frac{\Delta\Gamma}{\Delta m} = \frac{3}{2}\pi\frac{m_b^2}{m_t^2} \tag{22}$$

The time distribution for a decaying $\overline{B}^0$ meson originating from an initially produced B^0 state is given by:

$$\mathcal{P}(B^0_d \to \overline{B^0_d})(t) = \frac{1}{2}[1 - \cos(\Delta m_d\, t)] \exp\left(-\frac{t}{\tau(B^0_d)}\right) \tag{23}$$

A similar expression, but with a positive sign, describes the time distribution of a decaying B^0_d state. The parameter Δm_d, expressed in ps^{-1}, is the mass difference between the mass eigenstates of the $B^0_d - \overline{B^0_d}$ system. From this expression it is clear that a time dependent signal for oscillations can be observed only if one is able to tag the presence of a B^0_d or of a $\overline{B^0_d}$ at the time of the interaction and at the decay time of the meson. If not, the time distribution of the events is the usual exponential corresponding to the B^0_d lifetime. Integrating Equation (23) over the decay time, the probability to observe a $\overline{B^0_d}$ meson, starting from a B^0_d, is obtained:

$$\mathcal{P}(B^0_d \to \overline{B^0_d}) = \mathcal{P}(\overline{B^0_d} \to B^0_d) = \chi_d = \frac{[\Delta m_d\, \tau(B^0_d)]^2}{2 + [\Delta m_d\, \tau(B^0_d)]^2} \tag{24}$$

11.1 Before LEP

First signals for $B^0 - \overline{B}^0$ oscillations have been obtained in 1987 by detecting the presence of same sign dilepton events by ARGUS[3] [30] running at the $\Upsilon(4S)$ and by UA1 [31] at the $Sp\bar{p}S$. The latter signal was expected to receive contributions from B_d^0 and B_s^0 oscillations whereas the former was due only to the B_d^0.

11.2 Δm_d in year 2000

The first evidence for a time modulation of an oscillation signal was obtained by ALEPH [32] in 1993. It gives a direct access to the oscillation parameter Δm_d (see Equation (23)). Since that time, CDF, all LEP collaborations and SLD did 26 measurements which have been displayed in Figure 11-right. Averaging these measurements (http://lepbosc.web.cern.ch/LEPBOSC/), the obtained value can be compared with the corresponding result on χ_d, obtained at the $\Upsilon(4S)$ by ARGUS and CLEO collaborations.

$$\Delta m_d(\text{CDF, LEP, SLD}) = (0.486 \pm 0.015)\ \text{ps}^{-1},\ \Delta m_d(\Upsilon(4S)) = (0.489 \pm 0.032)\ \text{ps}^{-1}. \tag{25}$$

The overall average is then:

$$\Delta m_d(\text{ALL}) = (0.487 \pm 0.014)\ \text{ps}^{-1}. \tag{26}$$

In this last value the LEP weight is 70% (by end 2000).

This result has reached a 3% accuracy. An accurate determination of Δm_d is important to improve the determination of b-hadron production fractions (see Section 3) and to exploit at best the information provided by the search for $B_s^0 - \overline{B_s^0}$ oscillations (see Section 12).

12 Search for $B_s^0 - \overline{B_s^0}$ oscillations

The study of $B_s^0 - \overline{B_s^0}$ oscillations is much more difficult than for B_d^0 mesons because the $\overline{B_s^0}$ fraction in b-jets is close to 10% (a factor four smaller than for $\overline{B_d^0}$) and the oscillation period is expected to be shorter by a factor 20 ($\sim 1/\sin^2\theta_c$). The experimental resolution on the b-decay time plays an important role and this explains why SLD, in spite of a reduced registered statistics, as compared with LEP experiments, has a large weight in these analyses (50%).

The search for $B_s^0 - \overline{B_s^0}$ oscillations consists in analysing the decay time distribution of b-hadrons for two classes of events corresponding respectively to candidates classified as oscillating or as non-oscillating. The b or $\bar{b}$ content of the decaying hadron is usually defined by the charge of a lepton emitted at large transverse momentum relative to its jet axis.

The tagging at the production time makes use of the largest amount of accessible informations: average jet charge, charge of leptons or of kaons measured in the event's opposite hemisphere, charge of particles accompanying the b-decay products in its own hemisphere, ... Following the proposal explained in [33], the time distribution for the

[3] In ARGUS, they have also obtained evidence for oscillations by considering $B_d^0 - \ell$ correlations and by having a fully reconstructed event with two B_d^0 mesons.

signal has been modified as compared with Equation (23) by introducing a parameter, $\mathcal{A}$, called the oscillation amplitude:

$$\mathcal{P}(B_s^0 \to \overline{B_s^0})(t) = \frac{1}{2}[1 - \mathcal{A}\cos(\Delta m_s\, t)]\exp\left(-\frac{t}{\tau(B_s^0)}\right) \tag{27}$$

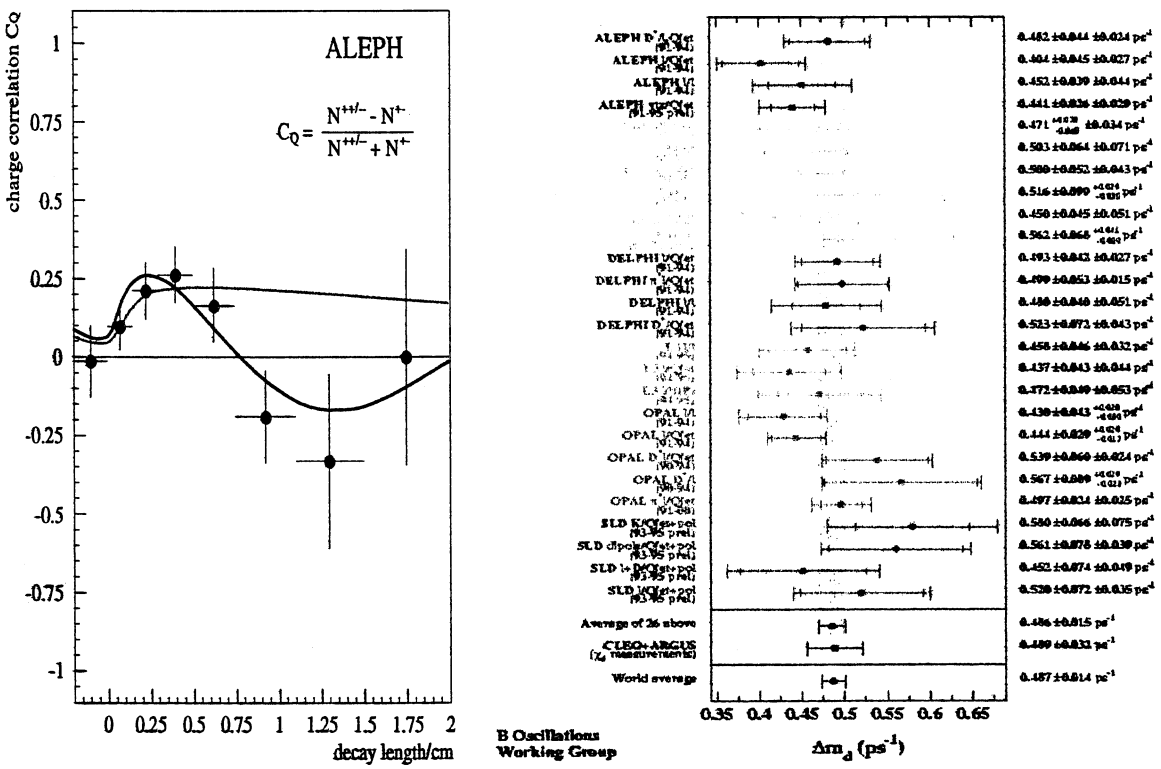

Figure 11: *Left: Experimental result of the charge correlation function C_Q. The result of the fit allowing for a time dependent oscillation is indicated by the solid line. The time independent alternative is shown by the other line. Right: Individual and combined measurements of Δm_d at LEP, CDF and SLD. The last average (Summer 2000) also includes χ_d measurements performed by CLEO and ARGUS experiments at the Υ(4S) resonance.*

The value of this quantity is measured on data for each assumed value of the oscillation parameter Δm_s. In the abscence of oscillation, at the corresponding value of Δm_s, the fitted value for $\mathcal{A}$ should be compatible with zero whereas, if the considered value of Δm_s corresponds exactly to the signal, $\mathcal{A}$ should be compatible with unity. For considered values of Δm_s, around the signal, $\mathcal{A}$ takes values between 0 and 1 and the expected distribution of $\mathcal{A}$, as a function of Δm_s, is a Breit-Wigner distribution, centred on the signal and of width equal to the inverse of the B_s^0 lifetime (neglecting resolution effects on the measured decay time). At present no significant signal for $B_s^0 - \overline{B_s^0}$ oscillations has been observed apart for a tantalizing 2.5 σ effect around 17.8 ps^{-1} (see Figure 12). From the averaged values of the amplitude and of its uncertainty, it is possible to define the value of Δm_s which is excluded with a 95% C.L.. It corresponds to the following equality:

$$\mathcal{A} + 1.645 \times \sigma_{\mathcal{A}} = 1. \tag{28}$$

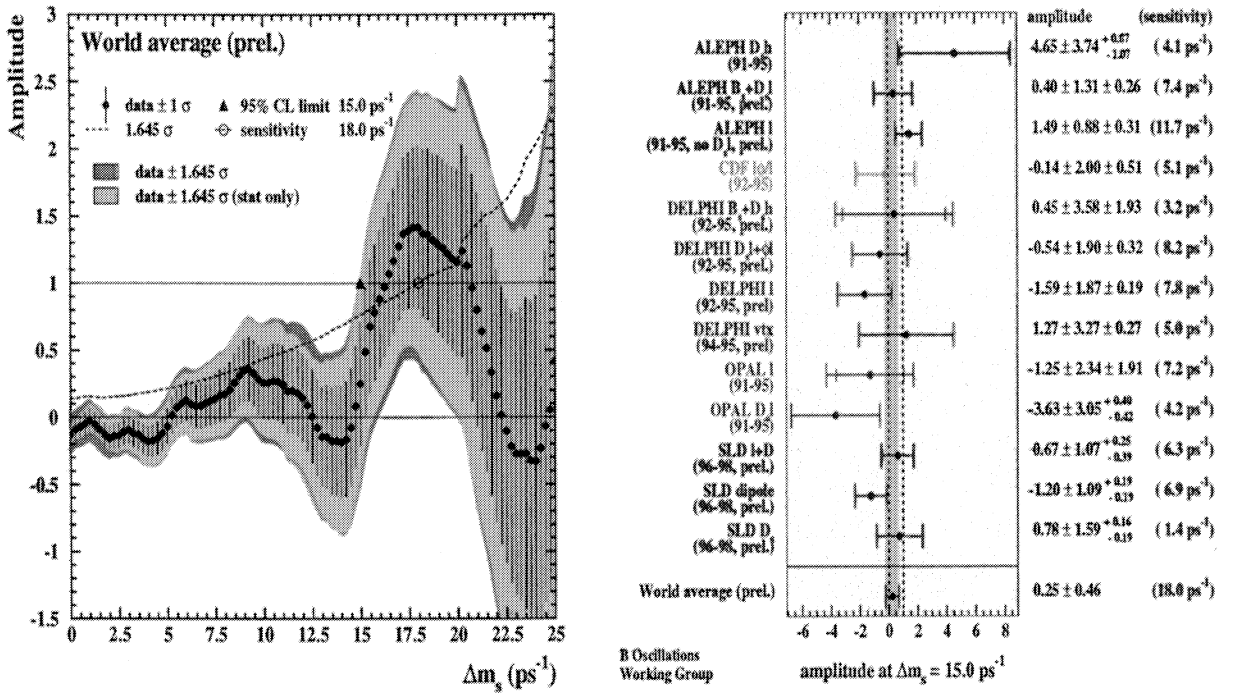

Figure 12: *Left: Combined B_s^0 oscillation amplitude as a function of Δm_s (by end 2000). A 95% C.L. lower limit on Δm_s of 15.0 ps^{-1} is derived from this spectrum. Points with error bars are the fitted amplitude values and corresponding uncertainties, including systematics. The dark (green) shaded area is obtained by multiplying these uncertainties by 1.645 such that the integral of the probability distribution, assumed to be Gaussian, is equal to 5% above this range. The light (yellow) shaded area is obtained in a similar way but including only statistical uncertainties in the fit; as a consequence, central values of the two regions do not necessarily coincide. Right: Measurements of the B_s^0 oscillation amplitude. The amplitudes are given at $\Delta m_s = 15$ ps^{-1}, along with the relevant statistical and systematic errors. The exclusion sensitivities are given within parentheses in the column on the right. Note that the individual measurements are as quoted in the original publications, but the average, corresponding to the hatched area, includes the effects of adjustments to a common set of input parameters. The dashed lines correspond to amplitude values of 0 and 1.*

The sensitivity of an analysis is defined by the same expression but considering that $\mathcal{A} = 0$. It is the expected limit in the absence of a signal. The increase of the sensitivity, versus time, obtained for combined LEP and SLD analyses is illustrated in Figure 13.

It goes from 6ps^{-1} in 1995, when LEP1 stops, to 18ps^{-1} in 2000. Improvements are still expected in 2001 and this may coincide also with the end of this activity, people having implemented all possible improvements in the various analyses. The actual limit on Δm_s, at 95% C.L., is lower than the sensitivity because of the possible signal mentioned already in the region of 18ps^{-1}. The variation of the fitted amplitude value with Δm_s is given in Figure 12-left whereas, in 12-right, are displayed the fitted amplitudes for the different analyses at the value $\Delta m_s = 15\mathrm{ps}^{-1}$. In these measurements, SLD has a 50% weight.

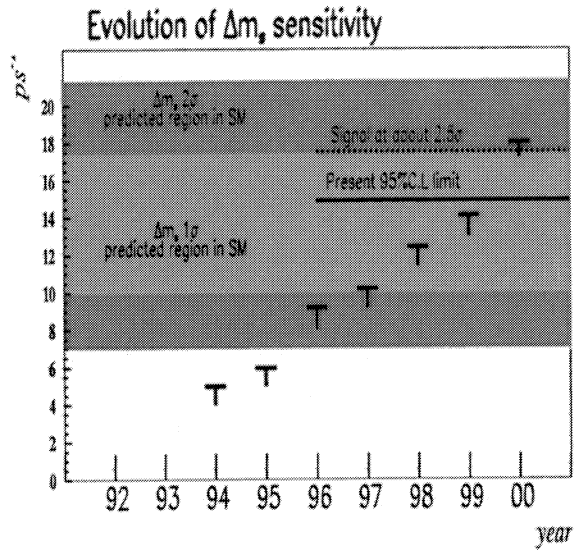

Figure 13: *Increase of the combined sensitivity of analyses searching for* $B_s^0 - \overline{B_s^0}$ *oscillations.*

13 Heavy hadrons decay constants

Decay constants of heavy-light quark-antiquark systems are contributing in many places of heavy quark physics (lifetime differences, oscillations) because they correspond to the overlap between the wave functions of the two quarks and thus to their possibility of annihilating or scattering by producing or exchanging, respectively, a virtual W boson.

13.1 Charm hadron decay constant

The leptonic decay of charged D hadrons can proceed through the weak annihilation of the constituent quarks (as in $\pi^- \to \ell^- \overline{\nu}_\ell$). As decaying mesons are pseudo-scalar and neutrinos are massless, it is an helicity suppressed mechanism. The total decay rate is:

$$\mathrm{BR}(\mathrm{P} \to \ell^+ \nu_\ell) = \frac{G_F^2}{8\pi} \tau(\mathrm{P}) f_\mathrm{P}^2 \left|V_{hq}\right|^2 m_\mathrm{P} m_\ell^2 \left(1 - \frac{m_\ell^2}{m_\mathrm{P}^2}\right)^2 \tag{29}$$

Typical values are given below:

$$\mathrm{BR}(\mathrm{D_s} \to \tau^+ \nu_\tau) = 4.9\%,\ \mathrm{BR}(\mathrm{D_s} \to \mu^+ \nu_\mu) = 0.5\%$$
$$\mathrm{BR}(\mathrm{D}^+ \to \tau^+ \nu_\tau) = 0.1\%,\ \mathrm{BR}(\mathrm{D}^+ \to \mu^+ \nu_\mu) = 0.04\%$$

Decay channels with a direct electron are suppressed because of the helicity. Present measurements are given in Figure 14-left. The most precise values have been obtained by ALEPH and CLEO. There is an intrinsic limitation in these measurements which comes from the uncertainty attached to the value of the production fraction of $\mathrm{D_s}$ mesons in

c-jets which is, itself, limited by the uncertainty of 25% attached to D_s decay branching fractions. The overall average corresponds to:

$$f_{D_s}(exp.) = (271^{+30}_{-34})\ \text{MeV}. \tag{30}$$

A compilation [34] of lattice QCD evaluations of f_{D_s}, done in the quenching approximation, is given in Figure 14-right. Recent evaluations have been performed, with limited statistics, also in the unquenched case:

$$\frac{f^{unquen.}_{D_s}}{f^{quen.}_{D_s}} = 1.09 \pm 0.14(MILC);\ 1.07 \pm 0.05(\text{CP} - \text{PACS}) \tag{31}$$

They seem to indicate an increase of the central value as compared with the unquenched determination. Considering a 10% increase and accounting for the corresponding uncertainty, the theoretical estimate becomes [34]:

$$f_{D_s}(lattice) = (250 \pm 25)\ \text{MeV}. \tag{32}$$

More precise determinations from lattice QCD are on the way. A better accuracy on experimental results, at the 1% level is possible at a Charm factory (and nowhere else). This will constitute an important test for these calculations if such measurements become available.

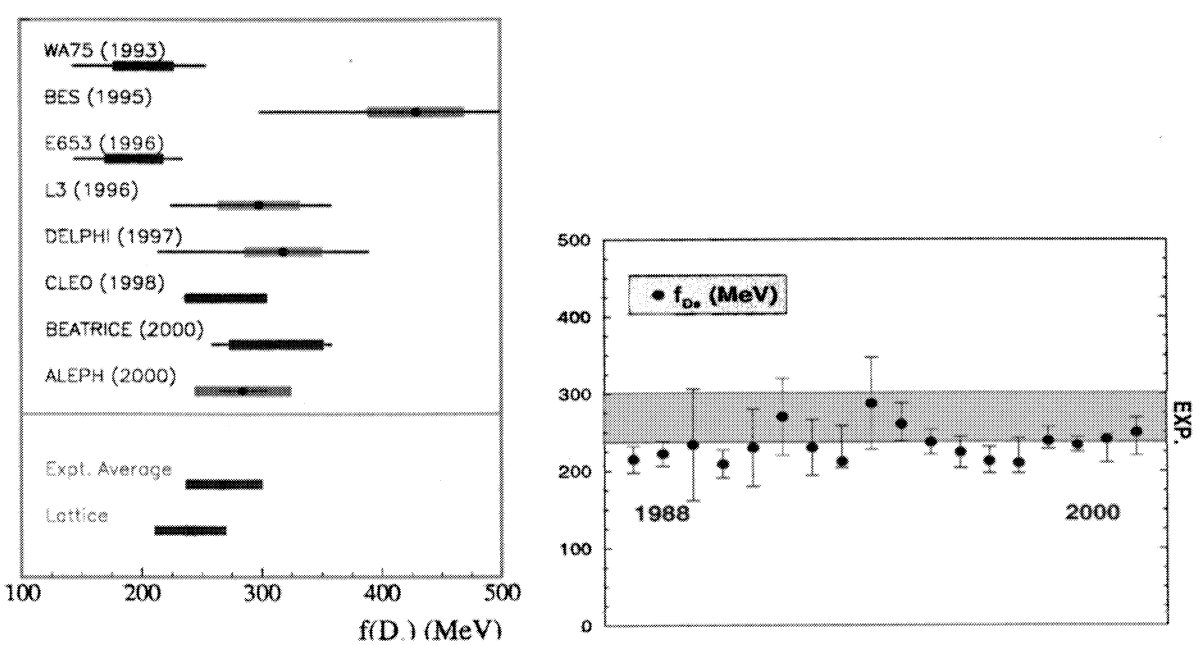

Figure 14: *Left: Present measurements of the D_s^+ decay constant. The thick and thin lines correspond respectively to systematic and statistic uncertainties. Right: Compilation of D_s^+ decay constant determinations by lattice QCD within the quenched approximation [34].*

13.2 B meson decay constant

I do not anticipate any measurement of leptonic B^+ decays in a nearby future. It may be easier to observe this decay channel for the B_c^+ in spite of the very small expected production rate for this particle at hadron colliders. An important difficulty will remain for evaluating an absolute branching fraction because of the very large uncertainty that will be attached to the B_c^+ production rate. The B^+ decay branching fraction is proportional to $(|V_{ub}| \times f_{B^+})^2$ and is thus expected to be rather small. Because of the background, this measurement requires, at B-factories, the reconstruction of the other B meson. The $\mu^+\nu_\mu$ channel may be more promising than the $\tau^+\nu_\tau$ because, in the former case, the muon is monochromatic in the B rest frame. Unfortunately the branching fraction is expected to be extremely small (helicity conservation).

Even if few events can be isolated, the parameter $|V_{ub}|$ is also rather uncertain giving an additional uncertainty in the determination of f_{B^+}. Most probably the determination of f_B will be obtained from lattice QCD once these calculations have been checked by comparing accurate determinations from theory with measurements for charmed mesons.

Another possibility consists in the measurement of the oscillation parameter for B_s^0 mesons, Δm_s, which can be expressed, in the Standard Model, as a function of $f_{B_s^0}\sqrt{B_{B_s^0}}$ and of known elements of the quark mixing matrix (see Section 23). In this approach, it has to be assumed that no new physics contributes to the value of Δm_s.

14 Charm counting in *b*-hadron decays

In the standard picture of weak decays of b-hadrons, through the emission or exchange of a virtual charged W boson, final states can contain zero, one or two charmed hadrons. As final states with no charmed hadron may originate from charmonium decays, corrections have to be applied to determine the fractions of events corresponding to one, two or no $c(\overline{c})$-quark present in the final state. The purpose of such studies is to examine if the total decay width of b-hadrons agrees with expectations and if the fraction of $0c$ events is not enhanced by new-phenomena. The expected fraction of double-charm events, which comes from the coupling of the virtual W to a $\overline{c}s$ pair, depends on the value assumed for the c-quark mass (because of phase-space limitations). As explained in Section 16, the semileptonic decay width of b-hadrons is considered to be in good theoretical control. The simultaneous measurement of the semileptonic branching fraction and of the average number of c-quarks, produced in b-hadron decays, allow then to constrain the theoretical description of inclusive b-hadron decays.

There are three experimental ways to measure the charm content of b-hadron decays: the counting of charmed hadrons, the inclusive analysis of the topologies of b- and c-decay vertices and the measurement of wrong-sign charmed hadron production [$BR(\overline{B} \to \overline{D}X)$]. The inclusive production of charmonium has also to be measured to correct the previous measurements, which depend only on D-hadron (open-charm) production, and have thus access to c-quark counting.

14.1 Charmonium production in *b*-hadron decays

Measured production rates for J/ψ and ψ' by CLEO and LEP experiments [2] are in agreement and have been averaged. Production rates of χ_c^1 and χ_c^2 have been only mea-

sured by CLEO [35] with sufficient accuracy. It has been assumed that these fractions are also applicable at LEP. It is necessary to correct the measured rates for cascade decays of higher charmonium states, this is indicated in Table 3.

Decay channel	measured rate (%)	direct production rate (%)	reference
BR($b \to J/\Psi X$)	1.153 ± 0.051	0.812 ± 0.064	CLEO/LEP average
BR($b \to \Psi' X$)	0.355 ± 0.049	0.355 ± 0.049	CLEO/LEP average
BR($b \to \chi_c^1 X$)	0.414 ± 0.051	0.383 ± 0.051	CLEO
BR($b \to \chi_c^2 X$)	0.10 ± 0.05	0.07 ± 0.05	CLEO

Table 3: *Charmonium production in b-hadron decays.*

Finally it is necessary to use models [36] to evaluate the contribution for not measured states as: χ_c^0, η_c and h_c. These rates have been estimated to be:

$$\mathrm{BR}(b \to \chi_c^0,\ \eta_c,\ h_c X) = (0.04 \pm 0.04)\%,\ (0.4 \pm 0.2)\%,\ (0.2 \pm 0.2)\% \qquad (33)$$

Quoted uncertainties, attached to these unknown rates, dominate the final uncertainty on charmonium production.

It must be noted that no theoretical model is able to explain the production rates of the different charmonium states. Colour singlet models are in agreement with the suppression of the χ_c^2 states relative to χ_c^1 but the global predicted rate is too low by an order of magnitude. Colour octet models can predict the observed rate but predict also more χ_c^2 than χ_c^1 production, at variance with the measurements.

The total branching fraction for charmonium production in b decays is thus:

$$n(c\bar{c}) = (2.3 \pm 0.3)\%. \qquad (34)$$

14.2 Open-charm counting

Inclusive production rates of D^0, D^+, D_s, Λ_c^+ and of their antiparticles have been measured in $b\bar{b}$ events at LEP and in $\Upsilon(4S)$ decays. Results have been summarized in Table 4. As B_s^0 and Λ_b^0 are produced in b-quark jets at LEP, the measured fractions of strange charmed mesons and of charmed baryons are higher than at the $\Upsilon(4S)$. The total measured charm production is rather similar in the two cases. It has to be noted the large uncertainties due to the poorly known values for D_s and Λ_c^+ branching fractions. In addition, contributions from strange charmed baryons have essentially to be guessed because

Decay channel	LEP	CLEO
BR($b \to D^0, \overline{D}^0 X$)	$(59.3 \pm 2.3 \pm 1.4)\%$	$(64.9 \pm 2.4 \pm 1.5)\%$
BR($b \to D^+, D^- X$)	$(22.5 \pm 1.0 \pm 1.5)\%$	$(24.0 \pm 1.3 \pm 1.6)\%$
BR($b \to D_s, D_s^- X$)	$(17.3 \pm 1.1 \pm 4.3)\%$	$(11.8 \pm 0.9 \pm 2.9)\%$
BR($b \to \Lambda_c^+, \overline{\Lambda}_c^- X$)	$(10.2 \pm 1.0 \pm 2.7)\%$	$(5.5 \pm 1.3 \pm 1.4)\%$

Table 4: *Measured production rates of charmed hadrons in b-hadron decays. The second quoted uncertainty is due to the error on charmed hadron branching fractions.*

there is not, at present, any absolute branching fraction measurement for these states. It is proposed to take:

$$\mathrm{BR}(\overline{\mathrm{B}} \to \Xi_c^{0,+}, \overline{\Xi}_c^{0,-}\mathrm{X}) = (0.4 \pm 0.3)\mathrm{BR}(\overline{\mathrm{B}} \to \Lambda_c^+, \overline{\Lambda}_c^-\mathrm{X})$$

in which the uncertainty corresponds to two extreme possibilities for the production of those states. The lower value corresponds to the usual suppression of strangeness production whereas the higher value corresponds to a possible enhancement of $\Xi_c^{0,+}$ production in events where the virtual $W^- \to \bar{c}s$ gives a strange quark in the final state that contributes directly to the creation of a Ξ_c baryon.

Including charmonium production, the average number of charm quarks produced in b-hadron decays is then:

$$n_c + n_{\bar{c}} = \sum_i (\mathrm{D_i \text{ or } \overline{D}_i})\mathrm{X} + 2n(c\bar{c}) = 1.144 \pm 0.059$$

where the uncertainty is dominated by those on charm particle absolute decay branching fractions.

14.3 Inclusive charm counting

Using their silicon vertex detectors, DELPHI [37] and SLD [38] have measured the fractions for $b \to 0\mathrm{D}$ and $b \to \mathrm{D}\overline{\mathrm{D}}$ (Table 5).

Experiment	BR($b \to$ 0D X)(%)	BR($b \to$ D $\overline{\mathrm{D}}$ X)(%)
DELPHI	$3.3 \pm 1.8 \pm 1.0$	$13.6 \pm 3.0 \pm 3.0$
SLD	$5.6 \pm 1.1 \pm 2.0$	$24.6 \pm 1.4 \pm 4.0$

Table 5: *Experimental results on no-open charm and two charm hadron branching fractions. The first uncertainty corresponds to statistical errors and un-correlated systematics whereas the second number is for correlated systematic uncertainties.*

The DELPHI analysis is based on the impact parameter distribution of charged particles relative to the beam interaction point. Figure 15 illustrates the different behaviour expected for different topologies of b-hadron decays.

The average between results from DELPHI and SLD gives:

$$\mathrm{BR}(b \to 0\mathrm{DX}) = (4.3 \pm 1.8)\% \quad (35)$$

$$\mathrm{BR}(b \to \mathrm{D}\overline{\mathrm{D}}\mathrm{X}) = (22.3 \pm 5.6)\%. \quad (36)$$

The quoted uncertainty in Equation (36) has been inflated to account for the poor agreement between the two double-charm rate measurements. From these values, it is possible to determine the average number of charm quarks emitted in b-hadron decays:

$$n_c + n_{\bar{c}} = 1 - \mathrm{BR}(b \to 0\mathrm{DX}) + \mathrm{BR}(b \to \mathrm{D}\overline{\mathrm{D}}\mathrm{X}) + 2n(c\bar{c}) = 1.183 \pm 0.042$$

The fraction of b-decays without any charm can be also determined by correcting for charmonium production, the measured rate for 0D production which includes this component:

$$\mathrm{BR}(b \to 0c\mathrm{X}) = \mathrm{BR}(b \to 0\mathrm{DX}) - n(c\overline{c}) = (2.0 \pm 1.8)\% \;\leftrightarrow\; (2.2 \pm 0.9)\%\ (\mathrm{Th.})$$

The measured value is in agreement with theoretical expectations [39] comprising only standard sources as: $b \to uX$ and $b \to s(d)g$. Models invoking a large component of b-hadron decays into non-charmed final states [40] are thus excluded.

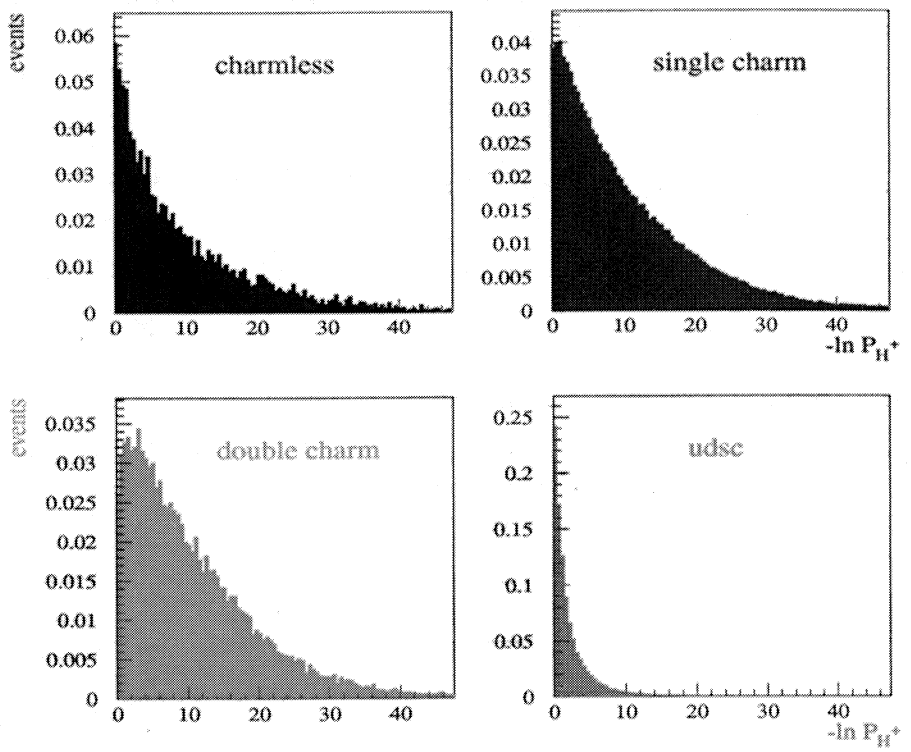

Figure 15: *The b-tagging probability distribution per hemisphere,P_H^+, from the 1994 simulation for charmless and hidden charm b-hadron decays, b-decays into one charm particle, b-decays into two open-charm particles, and the udsc background.*

14.4 Wrong-sign charm production

Another way to measure double charm production in b-hadron decays is to search only for wrong-sign charm production ($b \to \overline{\mathrm{D}}\mathrm{X}$). The rate for this process is the same as the rate for $b \to \mathrm{D}\overline{\mathrm{D}}\mathrm{X}$ apart for a tiny correction accounting for $b \to u$ transitions at the lower vertex [4]. Results obtained by ALEPH [41], CLEO [42] and DELPHI [43], using different techniques have been indicated in Table 6.

The analysis made by ALEPH [41] is based on the exclusive reconstruction of the two charmed hadrons emitted in the final state. An example is displayed in Figure 16.

[4]The $b \to c(u)W^-$ transition is usually named the lower vertex whereas the $W^- \to \overline{u}d(\overline{c}s)$ is referred as the upper vertex.

	$BR(\overline{B} \to \overline{D}X)$	$BR(\overline{B} \to D_s^- X)$	$BR(\overline{B} \to \overline{\Lambda}_c^- X)$
ALEPH	$0.094 \pm 0.032 \pm 0.006$	$0.148 \pm 0.035 \pm 0.043$	–
DELPHI	$0.090 \pm 0.022 \pm 0.002$	–	–
CLEO	$0.070 \pm 0.020 \pm 0.002$	$0.096 \pm 0.022 \pm 0.029$	0.008 ± 0.006
Average	0.082 ± 0.013	0.098 ± 0.037	0.008 ± 0.006

Table 6: *Probability of producing a charm hadron from the upper vertex in b-decays, accompanied by another charm particle emitted at the lower vertex, estimated from ALEPH, DELPHI and CLEO data, together with the average.*

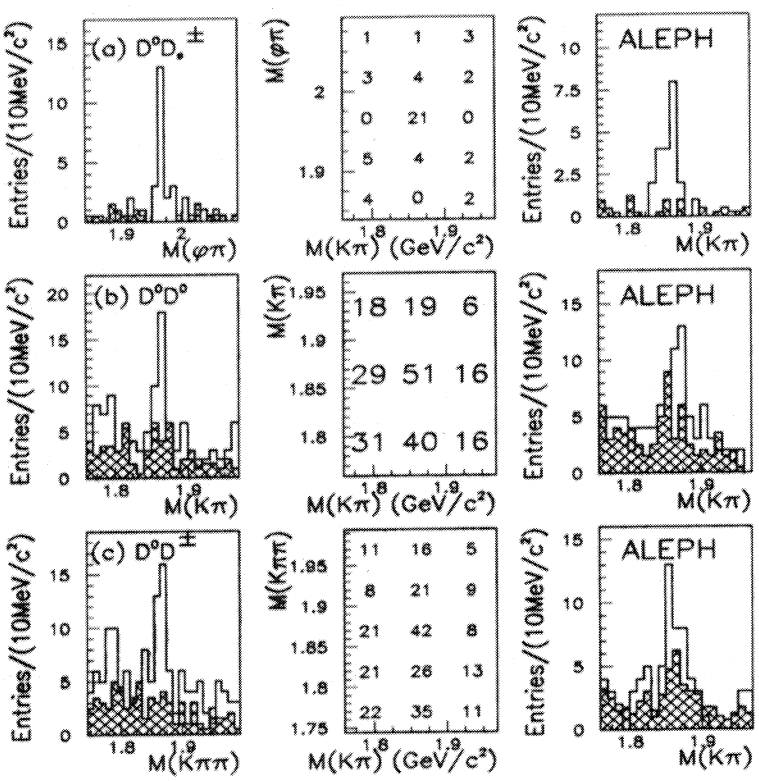

Figure 16: *The D_1 vs D_2 mass distributions for a few typical decay channels. The projection along $D_1(D_2)$ for $D_2(D_1)$ inside the D mass window is shown as an unshaded histogram. The shaded histogram is the projection along $D_1(D_2)$ for the average of upper and lower $D_2(D_1)$ sidebands, normalized to the surface of the signal region.*

14.5 Global average for charm production

The various results obtained in these three approaches can be averaged, taking into account correlated systematic uncertainties (as those coming from the determination of c-hadron decay branching fractions). The global average comprising results from ALEPH, CLEO, DELPHI, OPAL and SLD is:

$$n_c + n_{\overline{c}} = 1.206 \pm 0.033$$

15 Inclusive semileptonic branching fraction of b-hadrons

To measure the inclusive semileptonic branching fraction of b-hadrons it is necessary to distinguish between the different sources of leptons present in c- and b-quark jets as: $b \to \ell\, X$, $b \to c(\overline{c}) \to \ell\, X$ and $c \to \ell\, X$. This is obtained by using the different characteristics of the three channels: b-tagging, lepton transverse momentum relative to the jet axis, lepton isolation, ... These informations have been included in neural-networks to optimize the separation. The average of LEP measurements, obtained by the LEP Electroweak working group (http://lepewwg.web.cern.ch/LEPEWWG/), has changed with time as shown in Figure 17-left. This indicates that systematic uncertainties were not properly evaluated at some stage of these analyses. At present the LEP and CLEO values are rather similar. To compare the two results, LEP measurements have been slightly modified to correspond to the same sample composition (50% $\mathrm{B_d^0}$, 50% $\mathrm{B^+}$) as produced at the $\Upsilon(4S)$. This is done by assuming that all b-hadrons have the same semileptonic partial decay width and considering that differences between their semileptonic branching fractions come from differences in their total widths (or lifetimes). The equality of the semileptonic decay widths for $\mathrm{B^-}$ and $\overline{\mathrm{B_d^0}}$ mesons, corresponding to the $b \to c\ell^-\overline{\nu}_\ell$ transition, is strictly valid because of isospin invariance of strong interactions as the corresponding transitions correspond to ΔI=0. It has been assumed to be valid also for $\overline{\mathrm{B_s^0}}$ mesons and b-baryons. For b-baryons, an uncertainty of 15% has been added, estimated by comparing the lifetime ratios and semileptonic branching fraction ratios for b-mesons and b-baryons [44]. As a result, the inclusive semileptonic b-hadron branching fraction, measured at LEP, has been corrected according to the following expression:

$$\mathrm{BR}(b \to \ell^-\overline{\nu}_\ell X)(\mathit{corrected}) = \frac{\frac{1}{2}[\tau(\mathrm{B^+}) + \tau(\mathrm{B_d^0})]}{\tau_b}\mathrm{BR}(b \to \ell^-\overline{\nu}_\ell X). \tag{37}$$

Measured values for the inclusive branching fraction and for the number of charm quarks in b-hadron decays are compared with theoretical expectations [19] in Figure 17-right.

Present results favour a rather standard value for the charm quark mass and a low scale, μ, at which QCD corrections have to be evaluated:

$$\frac{m_c}{m_b} = 0.30 \pm 0.02, \quad \frac{\mu}{m_b} \sim 0.35 \tag{38}$$

16 Measurement of $|V_{cb}|$ in inclusive semileptonic b-hadron decays

The same formalism of O.P.E. can be used to evaluate the semileptonic partial decay width of b-mesons. Non-perturbative corrections are expected to contribute at the level of $\mathcal{O}(1/m_b^2,\ 1/m_c^2,\ 1/m_b m_c)$. To have a control of perturbative QCD corrections it is also important to work in a well defined renormalization scheme for quark masses [46]. This is because the m_b^5 dependence of the partial decay width amplifies the effects due to the running of quark masses if they are not compensated by other corrections in the matrix element. As an example the pole or $\overline{MS}$ definitions of quark masses are not appropriate

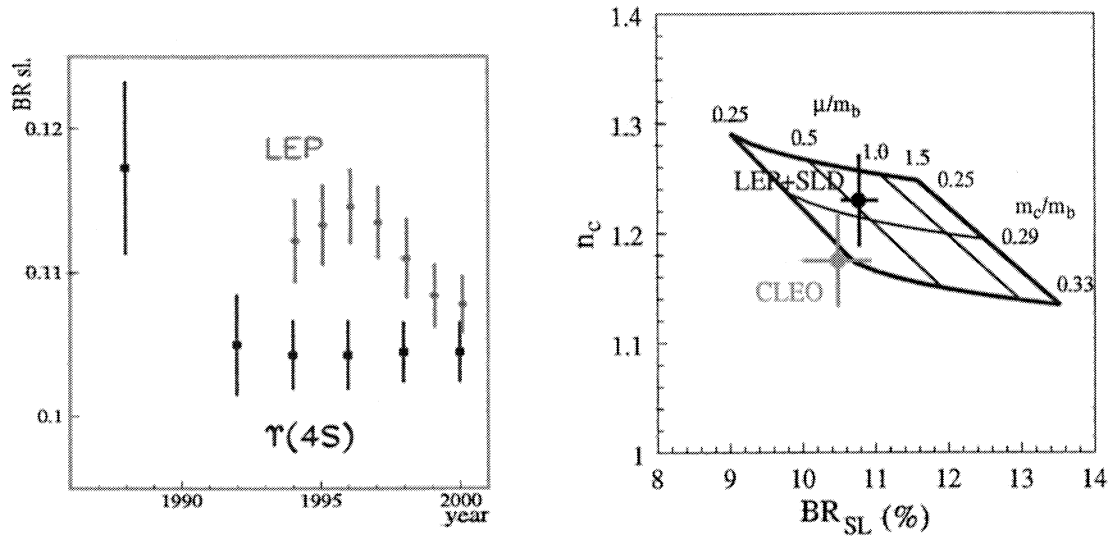

Figure 17: *Left: Time variation of the inclusive semileptonic b-hadron branching fraction measured at LEP and at the* $\Upsilon(4S)$. *The quoted numbers correspond to a sample containing the same fraction of* $\overline{B_d^0}$ *and* B^- *mesons. Right: Comparison between the measured number of c and* $\overline{c}$ *quarks in b-hadron decays and of the inclusive semileptonic branching fraction, with theoretical predictions. The value of the semileptonic branching fraction reported for CLEO is taken from [45].*

whereas the kinetic [46] or the 1S [47] masses give stable results. Values for the b-quark mass have been obtained using sum rules which relate the masses and the electronic decay widths of Υ mesons to moments of the vacuum polarization function [47, 48, 49]:

$$m_b^{kin.}(1GeV) = (4.58 \pm 0.06)\ GeV/c^2 \tag{39}$$

Within the same scheme it is possible to determine the difference between b- and c-quark masses:

$$m_b^{kin.}(1GeV) - m_c^{kin.}(1GeV) = \left[3.50 \pm 0.040\frac{\mu_\pi^2 - 0.5}{0.1} + \mathcal{O}(1/m_{b,c}^2)\right]\ GeV/c^2 \tag{40}$$

where μ_π^2 is the average momentum squared of the b-quark inside the b-hadron. Its value is estimated to be, at present: $\mu_\pi^2 = (0.5 \pm 0.1)\ GeV^2$ [50, 51].

The value of $|V_{cb}|$ is thus evaluated to be [52]:

$$|V_{cb}| = 0.0411\sqrt{\frac{BR(b \to X_c \ell^- \overline{\nu_\ell})}{0.105}}\sqrt{\frac{1.55\ ps}{\tau_b}}) \tag{41}$$

$$\times \left(1 - 0.012\frac{\mu_\pi^2 - 0.5}{0.1}\right) \tag{42}$$

$$\times \left(1 \pm 0.015_{pert.} \pm 0.010_{m_b} \pm 0.012_{1/m_Q^3}\right) \tag{43}$$

This corresponds to a relative error of 2.5% on $|V_{cb}|$. At present, it is considered as a safe approach [53], mainly because of the rather low value of the c-quark mass (of about

1 GeV/c^2) entering into these evaluations, to quote a 5% relative error and thus to double all previous numbers corresponding to the different uncertainties.

The extraction of $|V_{cb}|$, in this way, is based on the measurements of the inclusive b-hadron lifetime and semileptonic branching fraction. Present uncertainties on $|V_{cb}|$ are dominated by those from theory. In future, progress is expected from measurements of μ_π^2 by studying moments of the lepton momentum or of the mass of the hadronic system in b-hadron semileptonic decays.

17 Heavy quark masses

Values of heavy quark masses are scale and renormalization scale dependent. In this Section, values are given in the $\overline{MS}$ scheme.

17.1 The b-quark mass

Most precise determinations have been obtained by studying the Υ system and a summary is given in Figure 18-left. [54].

$$\overline{m_b}(\overline{m_b}) = (4.23 \pm 0.07)\ GeV/c^2 \tag{44}$$

Recently, at LEP and SLD, the evolution of this mass from the Υ to the Z mass scales has been observed (see Figure 18-right).

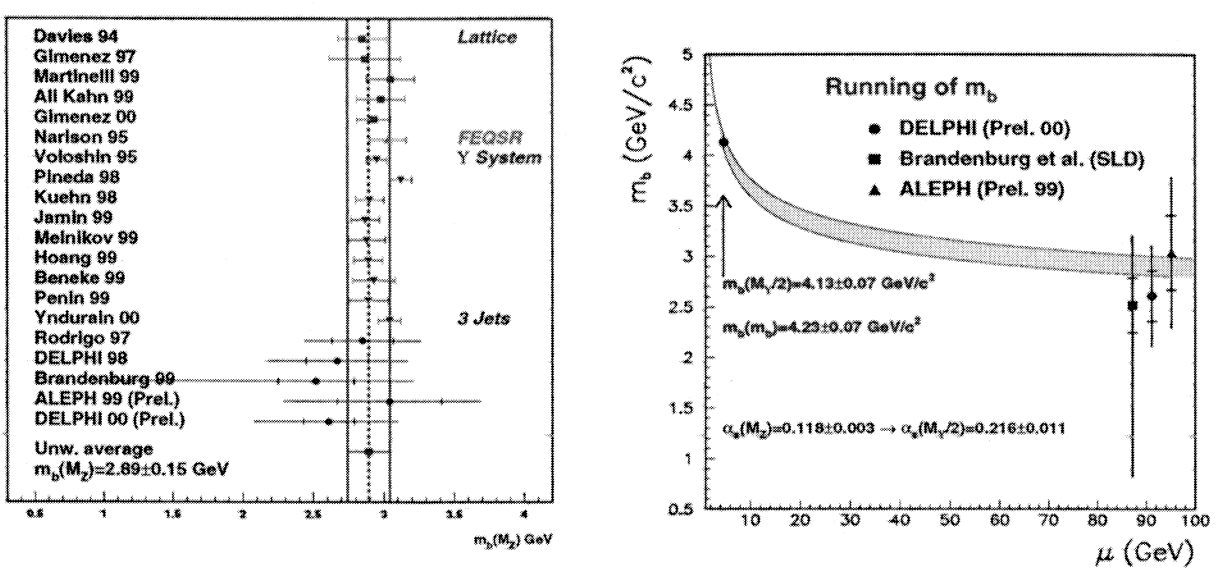

Figure 18: *Left: LEP, SLD and low energy results on $m_b(M_Z)$. Right: The running of $m_b(\mu)$ from the scale $M_\Upsilon/2$ up to the M_Z scale using the QCD renormalization group equations is compared with present measurements done at LEP and SLD.*

17.2 Other heavy quark masses

The c-quark mass has been also determined using QCD sum-rules applied to the J/ψ family [55]; a reasonable value seems to be:

$$\overline{m_c}(\overline{m_c}) = (1.23 \pm 0.09)\ GeV/c^2 \tag{45}$$

There is no contradiction between these values for the c- and b-quark masses and those mentioned in Section 16, used in the determination of $|V_{cb}|$. They correspond to determinations obtained in different renormalisation schemes and quoted values are consistent. Expressions relating the $\overline{MS}$ and the kinetic mass definitions can be found in [56].

The pole top quark mass has been measured by CDF and D0 collaborations at the TeVatron [57]: $M_t^{pole} = (174.3 \pm 5.1)$ GeV/c^2 [2]; it corresponds to:

$$\overline{m_t}(\overline{m_t}) = M_t^{pole}\left[1 - \frac{4}{3}\frac{\alpha_s(M_t^{pole})}{\pi} - ...\right] \simeq (167. \pm 5.)\ GeV/c^2 \tag{46}$$

18 b-meson exclusive semileptonic decays

In the following, the charged lepton mass is neglected and consequences of the Heavy Quark Effective Theory (H.Q.E.T.) are briefly explained.

18.1 $B^- \to D^0 \ell^- \overline{\nu_\ell}$

As the D^0 is a pseudo-scalar meson, the helicity of the virtual W^* is zero. In the centre of mass of the W^*, the charged lepton and the anti-neutrino are emitted back-to-back and, neglecting the mass of the charged lepton, are in an helicity state -1[5]. The distribution of the angle θ_l corresponding to the angle between the charged lepton and the D^0 meson directions in the W^* c.m. frame is thus proportional to: $(d^1_{0,-1})^2 \sim \sin^2\theta_\ell$. In addition, to conserve angular momentum, (as the D^0 as spin zero and the $\ell^-\overline{\nu_\ell}$ system is in J=1), a P-wave is needed between the D^0 and the $\ell^-\overline{\nu_\ell}$ system. The decay rate depends on a single form factor and thus can be expressed as:

$$\frac{d\Gamma}{dq^2} = \frac{G_F^2\,|V_{cb}|^2}{64\pi^4}\left|f_+(q^2)\right| p^{*3} \sin^2\theta_\ell \tag{47}$$

The mass squared of the $\ell^-\overline{\nu_\ell}$ is $q^2 = (p_\ell + p_{\nu_\ell})^2$ which has its maximum value when the D^0 meson is emitted at rest in the B^- rest frame, as indicated in Figure 19. In H.Q.E.T, the variable w, which is the product of the B^- and of the D^0 four-velocities, is introduced:

$$w = v_B \cdot v_D = \frac{m_B^2 + m_D^2 - q^2}{2m_B m_D} \tag{48}$$

and $w = 1$ corresponds to the maximum value for q^2. In this situation, where the heavy mesons are at rest, it is expected that strong forces do not notice the $b \to c$ transformation. A form factor is thus defined, which depends on w and which is normalized such that $\xi_D(1) = 1$. In terms of this form factor, the one previously introduced, can be written as:

$$f_+(q^2) = \frac{m_B + m_D}{2\sqrt{m_B m_D}}\xi_D(w) \tag{49}$$

[5]The helicity is measured by reference to the charged lepton direction.

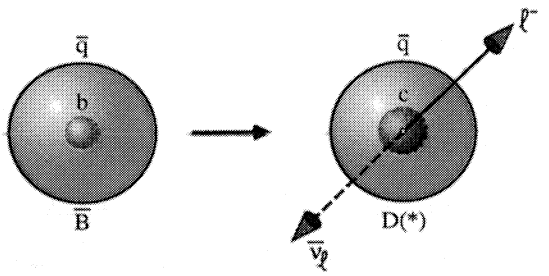

Figure 19: *Simplified description of the decay of a $\overline{B}$ meson for $q^2 = q^2_{max.}$.*

Corrections to unity of the value of this form factor, at $w = 1$, can be evaluated, and in case of $B^- \to D^0$ transitions, are expected to be of order $\mathcal{O}(1/m_Q)$.

18.2 $\overline{B^0_d} \to D^{*+}\ell^-\overline{\nu_\ell}$

As compared with the previous situation, the D^{*+} has spin 1 and the helicity of the W^* can be longitudinal (as in the previous case) and also transverse with $\lambda_{W^*} = \pm 1$. The decay angular distribution receives then additional contributing amplitudes and gets more complex. Three angles can be considered:

- θ_ℓ the angle between the directions of the charged lepton and of the W^*, in the $\ell^-\overline{\nu_\ell}$ rest frame,
- θ_D the angle between the directions of the D meson and of the D^{*+}, in the D^{*+} rest frame,
- χ the angle between the decay planes of the W^* and of the D^{*+}, in the $\overline{B^0_d}$ rest frame.

As in the previous decay, the helicity of the $\ell^-\overline{\nu_\ell}$ system is equal to -1 (neglecting the charged lepton mass). As the $\overline{B^0_d}$ is a spin 0 particle, the helicities of the D^{*+} and of the W^* have to be equal. Let's take, as an example, the evaluation of the decay amplitude corresponding to $\lambda_{W^*} = 1$.

The decay amplitude of the W^* will be proportional to:

$$d^1_{\lambda_{W^*},-1} = d^1_{1,-1} = \frac{1}{2}(1 - \cos\theta_\ell) \tag{50}$$

and the one corresponding to the D^{*+} decay to:

$$d^1_{\lambda_{D^{*+}},\lambda_{D^0}-\lambda_\pi} = d^1_{1,0} = -\frac{\sin\theta_V}{\sqrt{2}} \tag{51}$$

There are three form factors which can be, using H.Q.E.T., expressed in terms of a universal function $\xi_{D^{*+}}(w)$ and the decay rate becomes:

$$\frac{d(\mathrm{BR})}{dw} = \mathcal{K}(w)\xi^2_{D^{*+}}(w)\,|V_{cb}|^2\,;\ \xi_{D^{*+}}(1) = 1 \text{ if } m_{c,b} \to \infty \tag{52}$$

in which $\mathcal{K}(w)$ is a known function.

$$\mathcal{K}(w) = \frac{G_F^2}{48\pi^3} m_{D^*}^3 (m_B - m_{D^*})^2 \sqrt{w^2-1}(w+1)^2 \left(1 + \frac{4w}{w+1}\frac{1-2wr+r^2}{(1-r)^2}\right) \qquad (53)$$

with $r = m_{D^*}/m_B$. As compared with the previous case, it is expected that non-perturbative corrections to unity, for this form factor starts at order $\mathcal{O}(1/m_Q^2)$ and are thus under better control. The value used in the following will be [58]:

$$\xi_{\mathrm{D}^{*+}}(1) = 0.88 \pm 0.024 \frac{\mu_\pi^2 - 0.5}{0.1} \pm 0.035_{excit.} \pm 0.010_{pert.} \pm 0.025_{1/m^3} \qquad (54)$$

The variable μ_π^2 represents the square of the b-quark momentum within the b-hadron, it is expressed in GeV^2. In addition, using analyticity constraints, the complete w dependence of the universal form factor can be expressed in terms of its value and slope at $w = 1$ [59]. These two quantities can thus be fitted on data, once the variation of the decay rate has been measured as a function of w. This is illustrated in Figure 20 which gives distributions in which the experimental resolution has been unfolded. The upper plot corresponds to the measured decay rate which in practice goes to zero for $w \to 1$ whereas the lower plot gives the variation of the universal form factor.

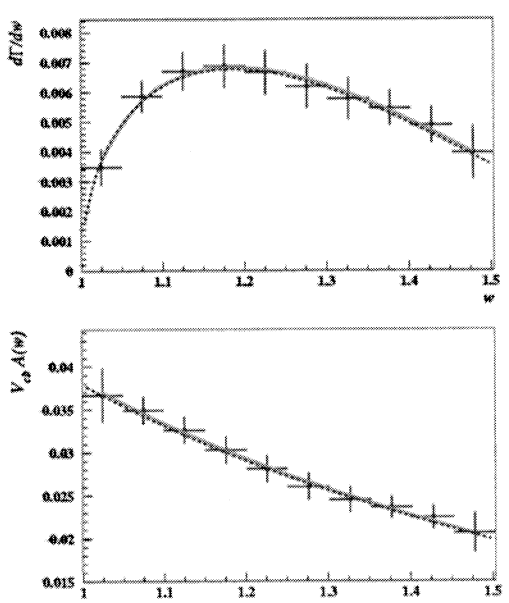

Figure 20: *DELPHI analysis [9]. Upper plot: differential decay width. Lower plot: decay form factor. The dotted line shows the results of a fit to the histograms, neglecting bin-to-bin correlations.*

19 $|V_{cb}|$ measurements at LEP

Fitted values for $\xi(1)\,|V_{cb}|$ and ρ^2 have been obtained by ALEPH [60], DELPHI [9] and OPAL [10] LEP collaborations. Their values are somewhat lower than a recent result

from CLEO [61] as indicated in Figure 21. The combined fit probability is 6%. This may indicate an underestimate of systematic uncertainties in one or in several analyses. It may be noted that the main systematic uncertainties are of different origins for CLEO and LEP experiments. At CLEO it comes from the determination of the efficiency to reconstruct the charged pion emitted in the D^{*+} decay as D^{*+} mesons are produced nearly at rest when w is close to unity. This is not a concern at LEP where D^{*+} mesons are fastly moving. The main uncertainty, at LEP, comes from the control of D^{*+} mesons emitted from D^{**} decays. This background is highly reduced at CLEO by cutting on the missing neutrino mass.

Exclusive and inclusive measurements of $|V_{cb}|$, obtained at LEP, have been combined [62] and give:

$$|V_{cb}| = (40.4 \pm 1.8) \times 10^{-3} \tag{55}$$

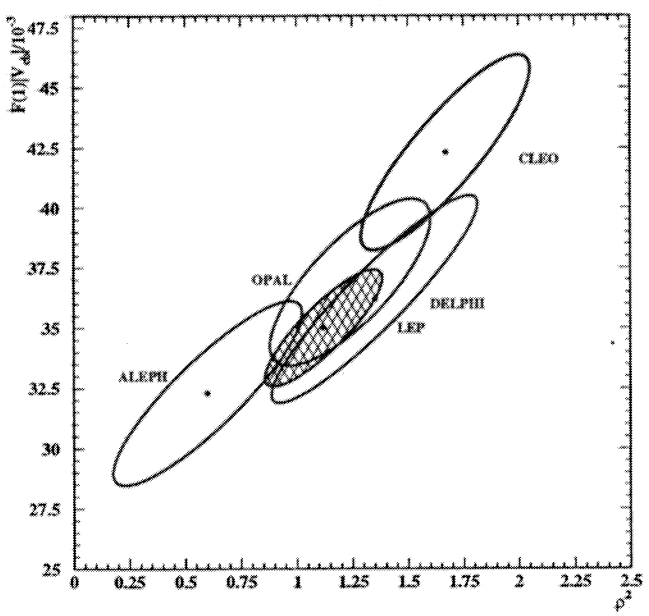

Figure 21: *Corrected measurements and LEP average of the quantities* $\xi(1)\,|V_{cb}|$ *and* ρ^2. *The error ellipses, centred on the different measurements, correspond to contours at the 68% C.L. level and include systematics. The hatched ellipse corresponds to the LEP average.*

20 Excited states in *b*-hadron semileptonic decays

Higher excited charmed states, corresponding to orbital or radial excitations, can be produced in *b*-hadron semileptonic decays. They will be called D^{**} in the following.

In terms of helicity form factors, the differential decay rate can be expressed in an universal way:

$$\frac{d\Gamma}{dw\ d\cos\theta_\ell} = \frac{G_F^2|V_{cb}|^2}{128\pi^3} m_D^2 m_B (w^2-1)^{1/2}(1+r^2-2rw) \tag{56}$$

$$\left[(1-\cos\theta_\ell)^2 H_+^2 + (1+\cos\theta_\ell)^2 H_-^2 + 2\sin^2\theta_\ell H_0^2\right] \tag{57}$$

where $r = m_D/m_B$. This expression is also valid for D and D* production. For the various "D" states, form factors are different and it remains to find, in the literature, the links between the helicity, the invariant, the HQET and the .... form factors.

The measurement of D** production in b-hadron semileptonic decays is difficult because of limited statistics at LEP and of the overlap between the two B decay products at CLEO or at b-factories.

An example of a semileptonic B^+, decaying into a D**, registered at LEP is shown in Figure 22.

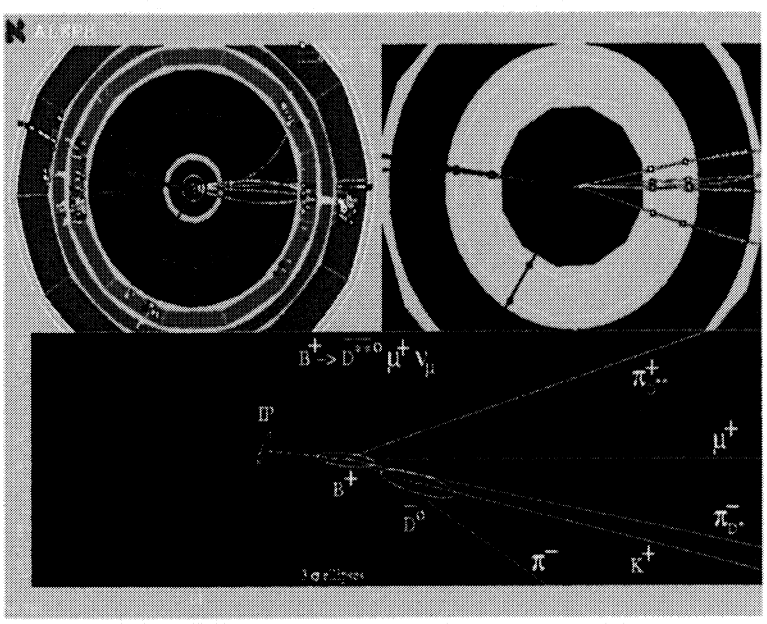

Figure 22: *Display of an ALEPH event which is candidate to correspond to the following decay chain:* $B^+ \to \overline{D}^{**0} \mu^+ \nu_\mu$, $\overline{D}^{**0} \to D^{*-} \pi^+$, $D^{*-} \to \overline{D^0} \pi^-$, $\overline{D^0} \to K^+ \pi^-$.

The analysis of these channels consists in identifying charged particle trajectories, different from the charged lepton and from the D or D* decay products, which are compatible with the position of the b-decay vertex and not compatible with the beam interaction point. Present results are summarized below [13]:

$$\mathrm{BR}(\overline{\mathrm{B}} \to \mathrm{D}_1 \ell^- \overline{\nu_\ell}) = (0.63 \pm 0.10)\% \quad (58)$$

$$\mathrm{BR}(\overline{\mathrm{B}} \to \mathrm{D}_2^* \ell^- \overline{\nu_\ell}) = (0.23 \pm 0.08)\% \text{ or } < 0.4\% \text{ at the 95\% C.L.} \quad (59)$$

$$\mathrm{R}^{**} = \frac{\mathrm{BR}(\overline{\mathrm{B}} \to \mathrm{D}_2^* \ell^- \overline{\nu_\ell})}{\mathrm{BR}(\overline{\mathrm{B}} \to \mathrm{D}_1 \ell^- \overline{\nu_\ell})} = 0.37 \pm 0.14 \text{ or } < 0.6 \text{ at the 95\% C.L.} \quad (60)$$

$$\mathrm{BR}(\overline{\mathrm{B}} \to \mathrm{D}_{broad}^{**} \ell^- \overline{\nu_\ell}) = (2.2 \pm 0.4)\% \quad (61)$$

The total semileptonic branching fraction into excited states is of the order of 30% of the total semileptonic decay rate. Present measurements are rather different from HQET expectations in the limit of heavy quarks of infinite mass [63]. In this limit it is expected that the narrow D** states ($\mathrm{D}_1, \mathrm{D}_2^*$) dominate over broad states and that the ratio between the D_2^* and the D_1 is of order 1.5. It appears that this ratio is lower than 0.6 at

95% C.L. and that non-narrow states have a two times larger production rate than the narrow states. This implies large $1/m_c$ corrections to these evaluations and measurements of the narrow states are in agreement with expectations that include such corrections [64]. In this model broad D^{**} states are still expected to be, at maximum, of the same order as narrow states. Present measurements imply that there is an additional non-resonant component of excited states.

21 Measurements of $|V_{ub}|$ at LEP

First signals of $b \to u$ transitions have been observed by CLEO in 1990. They correspond to leptons having a momentum higher than the end point for $b \to c\ell^-\overline{\nu}_\ell$ transitions. From this signal it is rather difficult to evaluate the total semileptonic branching fraction for $b \to u\ell^-\overline{\nu}_\ell$ because one is only sensitive to a small fraction of the decay rate corresponding to a peculiar region of the phase space. The measurements at LEP [65, 66, 67] consist in exploiting the topological differences between the two semileptonic channels. These experiments are sensitive to a large fraction of the decay phase space but the signal is situated over a large background which has to be controlled. An example is given in Figure 23-left which shows the lepton energy distribution evaluated in the b-hadron rest frame for a sample of events enriched in $b \to u$ decays.

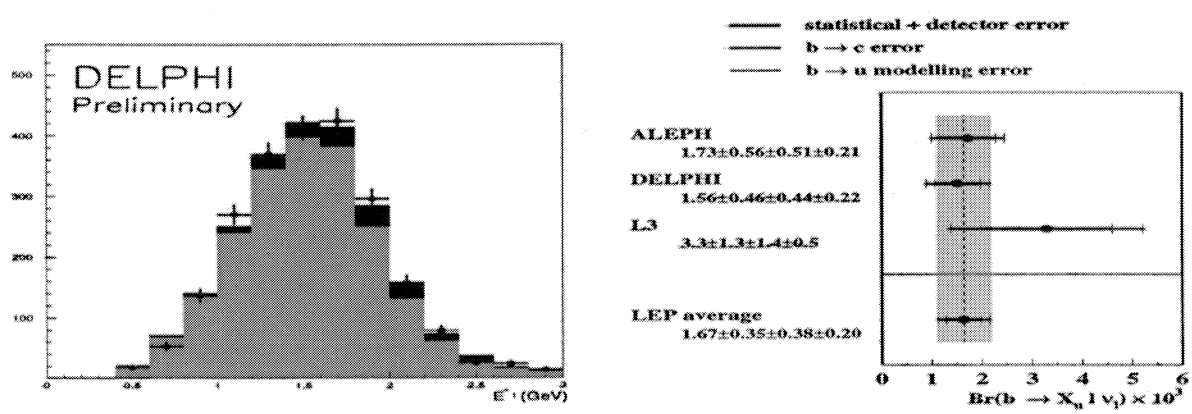

Figure 23: *Left: Distribution of the lepton energy in the b-hadron rest frame for the events sample enriched in $b \to u$ decays. Data are indicated by the points with error bars, the $b \to \ell^-\overline{\nu}_\ell X_u$ signal by the dark shaded histograms. Right: The determinations of $BR(b \to \ell^-\overline{\nu}_\ell X_u)$ at LEP and the resulting average (by Summer 2000).*

The value of $|V_{ub}|$ has been extracted using the following relationship derived in the context of (OPE) [68], [69]:

$$|V_{ub}| = 0.00445 \sqrt{\frac{\mathrm{BR}(b \to X_u \ell^-\overline{\nu_\ell})}{0.002}\frac{1.55\mathrm{ps}}{\tau_b}} \times \left[1 \pm 0.010(\mathrm{pert}) \pm 0.030(1/m_b^3) \pm 0.035(m_b)\right] \quad (62)$$

and:

$$|V_{ub}| = (4.13^{+0.63}_{-0.75}) \times 10^{-3} \text{ at the 68\% C.L.} \quad (63)$$

22 Quark mass matrices

It must be noted that this is not only Higgs physics but also a window on New Physics. Masses for fermions (and gauge bosons) are introduced in the Standard Model by Yukawa couplings to the Higgs field. The Lagrangian of weak interactions [70] contains several terms and among them there are:

- the weak charged current interaction with quarks:

$$\mathcal{L}_w = \frac{g}{\sqrt{2}} W_\mu^\dagger \overline{\mathrm{U}}_\mathrm{L} \gamma^\mu \mathrm{D}_\mathrm{L} \tag{64}$$

- quark mass terms:

$$\mathcal{L}_m = \left(\overline{\mathrm{U}}_\mathrm{L}^\mathrm{i} \;\; \overline{\mathrm{D}}_\mathrm{L}^\mathrm{i}\right) \Gamma_{ij} \begin{pmatrix} \phi^+ \\ \phi^0 \end{pmatrix} \mathrm{D}_\mathrm{R}^\mathrm{j} + \left(\overline{\mathrm{U}}_\mathrm{L}^\mathrm{i} \;\; \overline{\mathrm{D}}_\mathrm{L}^\mathrm{i}\right) \Delta_{ij} \begin{pmatrix} \phi^{0\dagger} \\ -\phi^- \end{pmatrix} \mathrm{U}_\mathrm{R}^\mathrm{j} \tag{65}$$

In this last expression Γ and Δ are general complex matrices.

After the spontaneous breaking of the symmetry: $<\phi^+>= 0$ and $<\phi^0> \neq 0$ and the quark mass terms become:

$$\mathcal{L}_m = \overline{\mathrm{D}}_\mathrm{L}\, \mathrm{M_D}\, \mathrm{D_R} + \overline{\mathrm{U}}_\mathrm{L}\, \mathrm{M_U}\, \mathrm{U_R} \tag{66}$$

in which:

$$\mathrm{M_D} = \Gamma \;\; <\phi^0>;\; \mathrm{M_U} = \Delta \;\; <\phi^0> \tag{67}$$

The quark-mass eigenstates are obtained by evaluating the diagonal mass matrices corresponding to $\mathrm{M_U}$ and $\mathrm{M_D}$. This is done by introducing unknown unitary transformations of the fields:

$$\mathrm{U'_R} = \mathrm{A_R^U U_R},\; \mathrm{U'_L} = \mathrm{A_L^U U_L},\; \text{and } \mathrm{U} \leftrightarrow \mathrm{D} \tag{68}$$

In this notation the physical u-quark, for instance, corresponds to: $u = \mathrm{U'_R} + \mathrm{U'_L}$.

The charged current weak interaction, expressed in terms of the quark-mass eigenstates becomes:

$$\mathcal{L}_w = \frac{g}{\sqrt{2}} W_\mu^\dagger \gamma^\mu \overline{\mathrm{U}}'_\mathrm{L} \mathrm{A_L^U} (\mathrm{A_L^D})^{-1} \mathrm{D'_L} = \frac{g}{\sqrt{2}} W_\mu^\dagger \gamma^\mu \overline{\mathrm{U}}'_\mathrm{L} \mathrm{V_{CKM}} D'_L \tag{69}$$

The CKM matrix is thus the product of two unknown unitary transformations entering in the diagonalisation of the up and down quark mass matrices.

As a result this matrix is unitary and depends a-priori on n_f^2 parameters, where n_f is the number of quark-lepton families. The physics is unchanged if the phases of the quark fields are modified:

$$\mathrm{U'_\alpha} \rightarrow \exp i\Psi_\alpha \; U'_\alpha,\; D'_\beta \rightarrow \exp i\Psi_\beta \; D'_\beta$$

This corresponds to the following transformation for the CKM matrix:

$$\mathrm{V}_{\alpha\beta} \rightarrow \exp i(\Psi_\alpha - \Psi_\beta)\; V_{\alpha\beta}$$

As there is an overall phase which is not observable, $2n_f - 1$ phases can be eliminated in this way.

As a result the CKM matrix depends on $(n_f - 1)^2$ parameters. For three families the four corresponding quantities comprise one phase implying that some of the matrix elements are complex quantities. As, for anti-quarks, one has to take the complex conjugate of the corresponding CKM elements, the presence of this phase in the matrix offers a mechanism for CP violation.

23 CKM matrix parametrization

The CKM matrix:

$$V_{CKM} = \begin{pmatrix} V_{ud} & V_{us} & V_{ub} \\ V_{cd} & V_{cs} & V_{cb} \\ V_{td} & V_{ts} & V_{tb} \end{pmatrix} \tag{70}$$

depends on three real and one imaginary quantities. There are several ways to introduce the complex phase in the matrix but the physics is independent of a peculiar choice. If other objects are contributing in weak transitions between different quark flavours, the interpretation of the measurements in terms of the unitary CKM matrix alone will be incorrect. It is thus expected to obtain incompatible results by doing different measurements of the same four parameters of the matrix. It is more likely that new physics contributes in mechanisms described by virtual loops as $P^0 - \overline{P}^0$ oscillations (P being K, D or B) or CP-violation through mixing reactions. New fields can contribute with new phases, inside these loops, and it has been anticipated that large deviations can be seen if one is able to measure directly the CP violation phase which can have a value rather different from expectations based on other measurements. In fact, for instance, when considering supersymmetry, the introduction of these new phases has such dramatic effects that one has also to introduce ad-hoc mechanisms to reduce such contributions so that the interpretation of present measurements (as CP violation in K physics) will not be completely spoiled.

Thus, in pratice, it is likely that deviations from Standard Model expectations on CP violation will be in fact rather small as it is the case, at present, for any other expected deviation induced by new physics. In addition, apart for very specific processes, all consistency tests of the unitarity of the CKM matrix are based on measurements which need a good control of non-perturbative QCD effects. At present such effects are controlled at the 10% level (about). In a near future a 1-few% accuracy can be obtained but it seems not realistic to expect a control at a level better than 1%. It seems to me rather unlikely that a few percent effects will be generated by new physics. b-factories will improve a lot our present knowledge on c- and b-meson decay properties and on several aspects of QCD but I do not expect that they find any new physics. New physics is in the hands of LHC or of neutrinos oscillation measurements or .....

In the Wolfenstein parametrization [71], the four parameters of the CKM matrix are named: λ, A, ρ and $i\eta$. They are defined by the following expressions:

$$V_{us} = \lambda;\ V_{cb} = A\lambda^2,\ V_{ub} = A\lambda^3(\rho - i\eta)$$

Considering that $\lambda \simeq 0.2$ is a small number, a developement in terms of powers of λ can be realized, valid up to $\mathcal{O}(\lambda^6)$:

$$\begin{pmatrix} 1 - \frac{\lambda^2}{2} - \frac{\lambda^4}{8} & \lambda & A\lambda^3(\rho - i\eta) \\ -\lambda + \frac{A^2\lambda^5}{2}(1 - 2\rho) - iA^2\lambda^5\eta & 1 - \frac{\lambda^2}{2} - \lambda^4(\frac{1}{8} + \frac{A^2}{2}) & A\lambda^2 \\ A\lambda^3\left[1 - (1 - \frac{\lambda^2}{2})(\rho + i\eta)\right] & -A\lambda^2(1 - \frac{\lambda^2}{2})\left[1 + \lambda^2(\rho + i\eta)\right] & 1 - \frac{A^2\lambda^4}{2} \end{pmatrix}$$

23.1 Measurements of the parameters λ and A

The $|V_{ud}|$ and $|V_{us}|$ elements, which depend on λ, are measured respectively by studying transitions in nuclei and K weak decays. At present there is a two sigma difference between

different determinations and we will use:

$$\lambda = 0.2237 \pm 0.0033 \leftrightarrow 0.2196 \pm 0.0023 \ (PDG\ 2000)$$

The parameter λ is equal to $\sin\theta_c$ where θ_c is the usual Cabibbo angle.

By definition $|V_{cb}| = A\lambda^2$ and, as explained in Section 16, semileptonic decays of b-hadrons are used to determine this quantity which is known with an uncertainty of the order of 5% (of theoretical origin).

23.2 Constraints on the two other parameters: ρ and $i\eta$

The unitarity of the CKM matrix provides six expressions corresponding to products of two lines or two columns which can be vizualized, in a complex plane by triangles. In practice, there is only one of these triangles which has sides of similar lengths. It corresponds to the following expression:

$$V_{ud}^* V_{ub} + V_{cd}^* V_{cb} + V_{td}^* V_{tb} = 0$$
$$\overline{AC} = \frac{1-\lambda^2/2}{\lambda}\left|\frac{V_{ub}}{V_{cb}}\right| \qquad \overline{AB} = \frac{1}{\lambda}\left|\frac{V_{td}}{V_{cb}}\right|$$

All sides have a length of order $A\lambda^3$ which is used to rescale all lengths before doing a display in the $(\rho, i\eta)$ plane. The summits of the triangle are situated in this plane at the following positions: A(0,0), C$(\rho, i\eta)$ and B(1,0). It may be noted that, as $(A\lambda^3)^2$ is a rather small number, some of the processes of interest to test the unitarity of the CKM matrix will require a very large number of produced b-hadron decays.

At present there are four measurements, indicated in Table 7, which can be used to constrain the region of possible values for ρ and $i\eta$. In these expressions, the quantities: $\bar{\rho} = \rho(1-\lambda^2/2)$ and $\bar{\eta} = \eta(1-\lambda^2/2)$ have been introduced [72]. In the following sections, the analysis done in [73] has been summarized.

Measurement	$V_{CKM}\times$other	Constraint
$b \to u / b \to c$	$\lvert V_{ub}/V_{cb}\rvert^2$	$\bar{\rho}^2 + \bar{\eta}^2$
Δm_d	$\lvert V_{td}\rvert^2 f_{B_d}^2 B_{B_d} f(m_t)$	$(1-\bar{\rho})^2 + \bar{\eta}^2$
$\frac{\Delta m_d}{\Delta m_s}$	$\left\lvert\frac{V_{td}}{V_{ts}}\right\rvert^2 \frac{f_{B_d}^2 B_{B_d}}{f_{B_s}^2 B_{B_s}}$	$(1-\bar{\rho})^2 + \bar{\eta}^2$
ϵ_K	$f(A, \bar{\eta}, \bar{\rho}, B_K)$	$\propto \bar{\eta}(1-\bar{\rho})$

Table 7: *The four constraints which can be used, at present, to determine the favoured values for the parameters ρ and $i\eta$. Complete expressions for these constraints can be found, for instance in [73].*

23.3 Unitarity test before b-factories

In addition of improving the determinations of the lengths of the unitarity triangle sides, b-factories will also measure the angles of the triangle (mainly β in practice). But, before considering their results, it is already possible to compare measurements of the sides (deduced from results obtained at CDF, CLEO, LEP and SLD), with the constraint coming from CP violation in Kaon physics. The measurement of ϵ_K selects a band centred on an

hyperbola in the $(\rho, i\eta)$ plane. Contours corresponding to the combined measurements of $\left|\frac{V_{ub}}{V_{cb}}\right|$, Δm_d and Δm_s are also drawn in Figure 24. As can be seen the two types of constraints, obtained respectively in K and B physics, are in agreement. This gives already a test, with accuracy limited to ± 0.20, of the coherence of the CP-violation picture provided by the Standard Model.

Hatched areas corresponding to direct measurements of $\sin(2\beta)$ at b-factories and other facilities are also displayed. They correspond to the following average value: $\sin(2\beta) = 0.49 \pm 0.16$ (by Summer 2000).

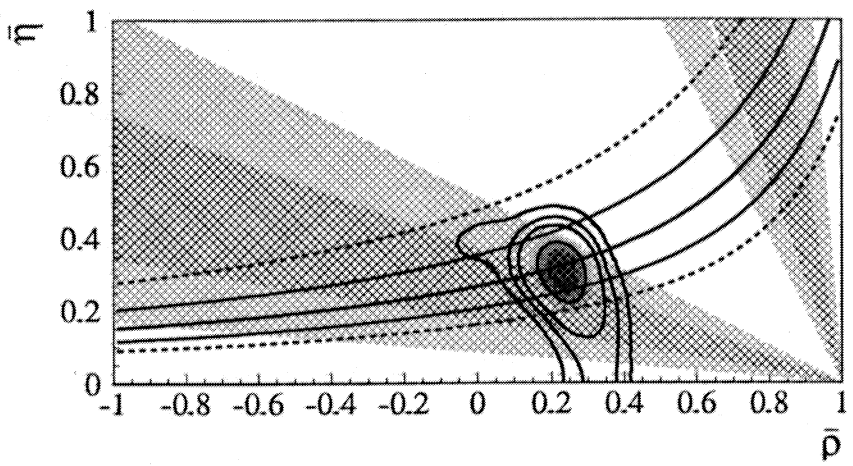

Figure 24: *The allowed regions (at 68%, 95%, 99% and 99.9% probability) for $\overline{\rho}$ and $\overline{\eta}$ using the constraints given by the measurements of $\frac{|V_{ub}|}{|V_{cb}|}$, Δm_d and Δm_s. The constraint related to $|\epsilon_K|$ is not included. The regions (at 68% and 95% probability) selected by the measurements of $|\epsilon_K|$ [continuous (1σ) and dotted (2σ) curves] and $\sin(2\beta)$ [darker (1σ) and clearer (2σ) zones] are shown. For β, the two solutions are displayed.*

23.4 Measurements of the CKM triangle parameters before *b*-factories

Combining the four constraints, values for ρ, η and for the angles of the triangle have been obtained. These values are given in the hypothesis that the S.M. gives the correct expressions for the different constraints. It has been already noted that there is no indication (within $\pm 0.1 - 0.2$) that the different constraints are not compatible. Another test will consists in comparing values of $\sin(2\beta)$ obtained in this way with direct measurements at b-factories.

Figure 25 gives the present favoured region which corresponds to:

$$\bar{\rho} = 0.224 \pm 0.038; \ \bar{\eta} = 0.317 \pm 0.040$$

Probability distributions for the expected values of the α and β angles are illustrated in Figure 26 and correspond to:

$$\sin(2\beta) = 0.698 \pm 0.066, \ \ \sin(2\alpha) = -0.42 \pm 0.23 \qquad (71)$$

The angle β is rather well determined as all contributing constraints overlap.

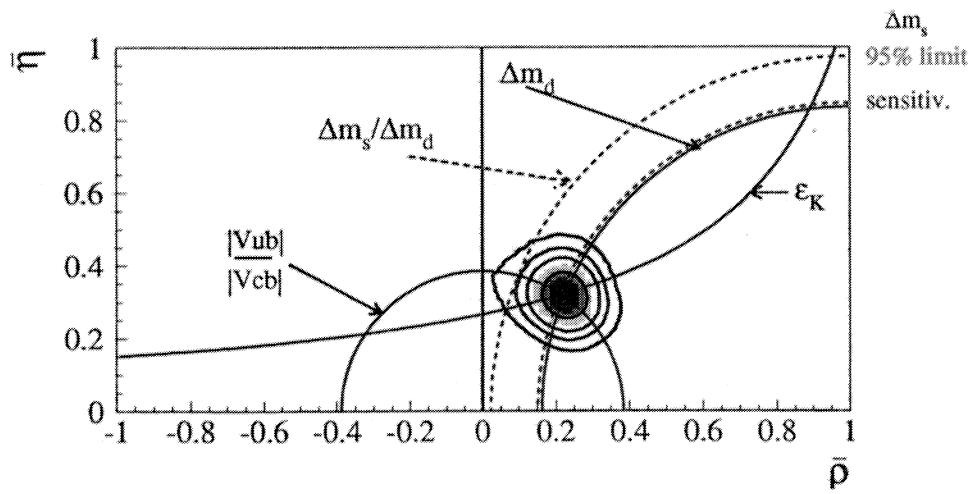

Figure 25: *Allowed regions for $\overline{\rho}$ and $\overline{\eta}$ as obtained in [73]. The contours at 68%, 95%, 99% and 99.9% probability are shown. The full lines correspond to the central values of the constraints given by the measurements of $\frac{|V_{ub}|}{|V_{cb}|}$, $|\epsilon_K|$ and Δm_d. The two dotted curves correspond, from left to right respectively to the 95% upper limit and to the value of the exclusion sensitivity obtained from the experimental study of $B_s^0 - B_s^0$ oscillations.*

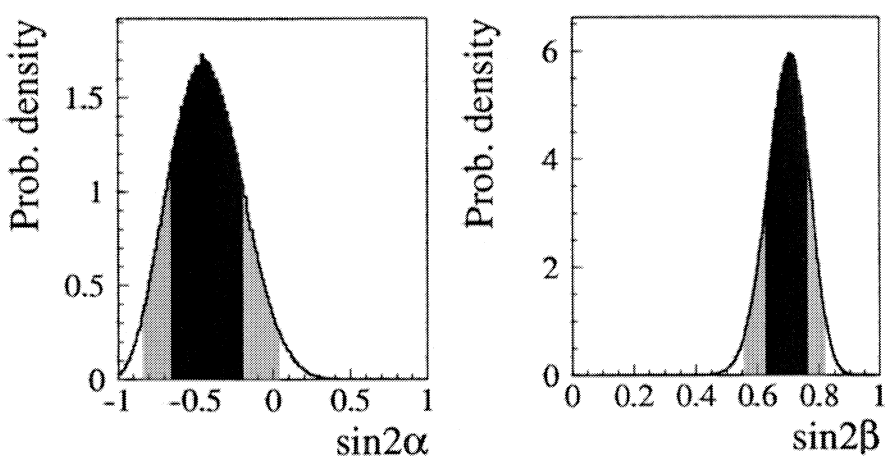

Figure 26: *The p.d.f. for* $\sin(2\alpha)$ *and* $\sin(2\beta)$. *The darker and the clearer zones correspond respectively to 68% and 95% of the normalised area.*

The angle γ is also rather precisely defined (see Figure 27) as the search for $B_s^0 - \overline{B_s^0}$ oscillations eliminates completely the region corresponding to $\gamma > 90°$. Upper limits on γ are also given by the other constraints. As a result:

$$\gamma = (54.8 \pm 6.2)° \text{ and } \gamma > 90° \text{ at } 0.03\% \text{ C.L.}$$

Analyses on $B_s^0 - \overline{B_s^0}$ oscillations play a major role in this result.

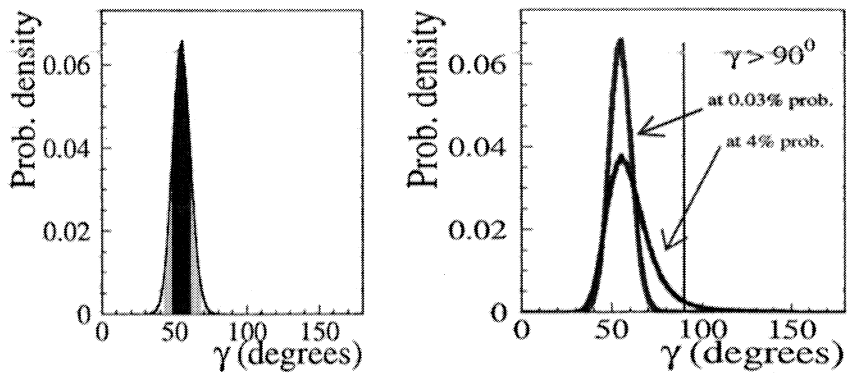

Figure 27: *Left: the p.d.f. for γ. The darker and the clearer zones correspond respectively to 68% and 95% of the normalised area. Right: the same p.d.f. is drawn when the constraint coming from the limit on Δm_s is not included.*

23.5 Present anomalies or expectations

The value obtained for γ has already interesting consequences. In the framework of the factorization approach, two-body decays of $\overline{B_d^0}$ and B^- mesons have been analyzed by several authors. Figure 28 illustrates a few predictions from these models as a function of the value of the angle γ [74].

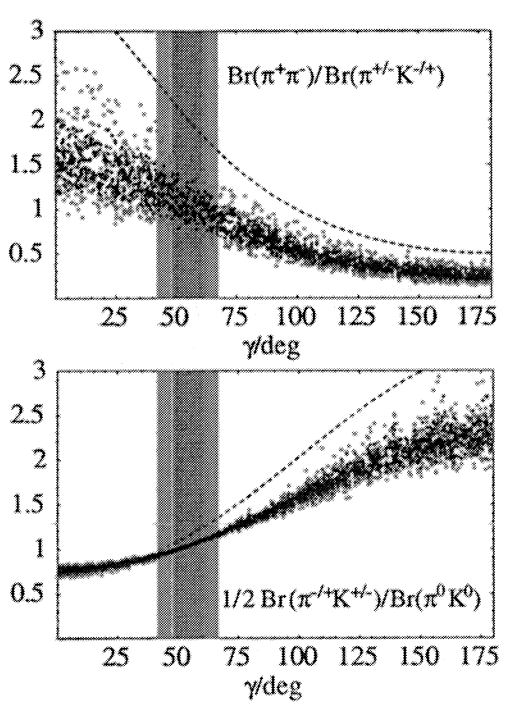

Figure 28: *Theoretical predictions [74] for two CP-averaged branching fraction ratios of charmless b-hadron decays. Dark dots correspond to a "realistic" scan of values for the input parameters and clearer dots cover a more conservative domain. The dashed line is the prediction for conventional factorization. The vertical bands represent the fitted value for the angle γ as given previously.*

Present measurements obtained at CLEO, BaBar and BELLE, of the corresponding CP-averaged ratios are:

$$\frac{\mathrm{BR}(\pi^+\pi^-)}{\mathrm{BR}(\pi^{+/-}\mathrm{K}^{-/+})} = 0.26 \pm 0.06; \quad \frac{1}{2}\frac{\mathrm{BR}(\pi^{+/-}\mathrm{K}^{-/+})}{\mathrm{BR}(\pi^0\mathrm{K}^0)} = 0.83 \pm 0.22$$

It is quite apparent, that measured values for these ratios favour essentially disconnected regions: large values of γ for the first ratio and rather low for the second. If one discards possible experimental artefacts, it is the theoretical formalism which is questionnable. A more recent and detailed analysis [75] gives a better agreement with experimental results but it is still difficult to accomodate the value of γ given in Equation (72) with the first ratio. Such discrepancies have to be analyzed in more details to infer informations on the validity of QCD analyses of two-body charmless b-meson decays.

Without including the constraint from $\mathrm{B}_s^0 - \overline{\mathrm{B}_s^0}$ oscillations, the favoured region for the value of Δm_s is given in Figure 29-left. Including all constraints a rather narrow region is isolated at 95% probability between 15.6 and 20.5 ps^{-1}. Very large values of Δm_s are not expected and there is a good chance that this parameter will be measured soon by CDF at the TeVatron.

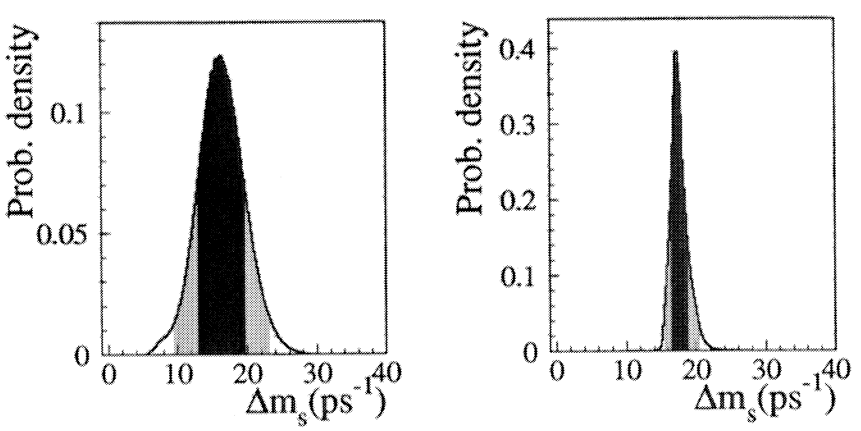

Figure 29: *Left: the p.d.f. for Δm_s obtained from all constraints but the one obtained from analyses on the $B_s^0 - \overline{B_s^0}$ system. The darker and the clearer zones correspond respectively to 68% and 95% of the normalised area. Right: the same p.d.f. is drawn when all constraints are applied.*

In a similar way it is possible to remove, in turn, the constraint from Δm_d and $|\epsilon_K|$ measurements and to predict the expected values for the theoretical parameters which enter in the interpretation of these measurements, within the S.M.. A good consistency is observed (Table 8).

23.6 Evolution of the allowed (ρ, η) plane region

It maybe interesting to illustrate what has been learned during the past 10 years concerning the allowed region for the parameters ρ and η. This is illustrated in Figure 30.

Before 1988, $|\mathrm{V}_{cb}|$ was determined with 20% error and there was no experimental result on $b \to u$ transitions. The upper limit on η was, consequently rather weak. It was

Parameter	Input value (lattice)	Fitted value
B_K	$0.86 \pm 0.06 \pm 0.13$	$0.90^{+0.30}_{-0.14}$
$f_B\sqrt{B}$	$220 \pm 20 \pm 25\ MeV$	$231 \pm 15\ MeV$

Table 8: *Comparison between the expected values of B_K and $f_B\sqrt{B}$ obtained from lattice QCD and the values which are favoured by all constraints but the one which depends on these quantities.*

obtained from the theoretical interpretation of the inclusive semileptonic decay branching fraction of b-hadrons in terms of the two components: $b \to u$ and $b \to c$ transitions. The b-hadron lifetimes were essentially unmeasured and B_K was expected to be between 1/3 and 1. Essentially no-constraint can be imposed on ρ and $i\eta$.

In 1987-88 first results on $B^0_d - \overline{B^0_d}$ oscillations were available and also theoretical determinations of $f_B\sqrt{B}$ with 30% error. These results implied that the top quark must be heavy. First results on $|V_{ub}|$ were obtained with 50% error. This corresponds to the upper plot in Figure 30.

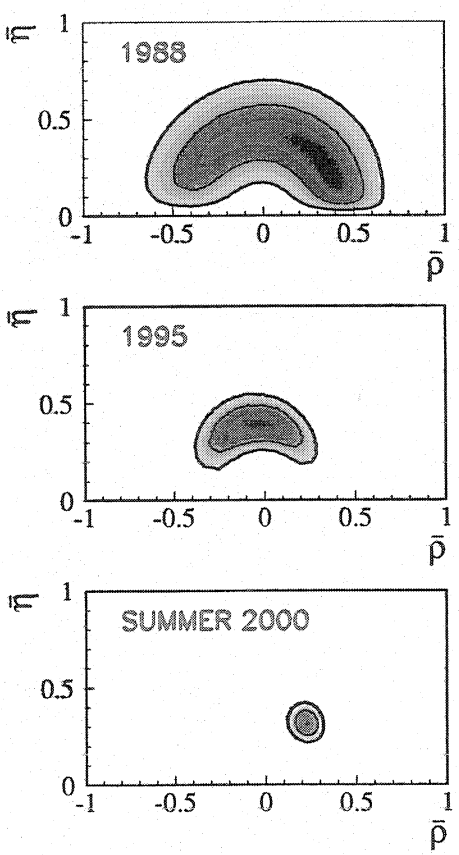

Figure 30: *Variation of the allowed region in the (ρ, η) plane. The two contours, drawn on each plot, correspond respectively to 68 and 95% probability regions.*

In 1994-95 main improvements come from the direct determination of the top quark mass, a 10% uncertainty on $|V_{cb}|$, evaluations of B_K in lattice QCD with 25% error, Δm_d

known with 5% uncertainty and from the b-lifetime measurements with 2% error.

Finally now, limits on Δm_s have been enormously improved during the past five years and we benefit also from large improvements in the accuracy of lattice QCD evaluations for the parameters B_K, $f_B\sqrt{B}$ and ξ, giving a determination of the parameters $\sin(2\beta)$ and γ with a 10% error, within the S.M. framework.

24 Conclusions

My purpose, in these two lectures, was to give an overall picture of the progress made during the last few years in the determination of b-hadron properties and to indicate how these studies have improved our understanding of the Standard Model description of the sector of flavour.

For Summer conferences, this year (2001), the BaBar and BELLE collaborations have obtained the first significant results on CP violation in the $B^0_d - \overline{B^0_d}$ system. Averaging these new measurements with previous indications from CDF and LEP gives:

$$\sin(2\beta) = 0.82 \pm 0.13 \tag{72}$$

This value is in agreement with the one quoted in Equation (71) which was obtained, independently, from measurements of the sides of the triangle, from the constraint from CP violation in K-physics and from lattice QCD. It thus confirms the Standard Model picture of CP violation. This result has also an important consequence because it implies that it will be difficult to observe, at b-factories, a significant deviation of $\sin(2\beta)$ due to effects from new-physics[6]. This does not mean that non-standard-model effects on CP violation phases do not exist. Maybe it will be wise to wait for direct new-physics signals from LHC to have a better idea on the real importance of such effects and on the channels that will be most promizing to see deviations from S.M. expectations. In the meantime, detailed studies of b-hadrons at b-factories and hadron-colliders and of c-hadrons at Tau/Charm factories, will provide accurate validation tests for QCD technologies, as lattice QCD, in the non-perturbative domain. From these studies it is expected to get more accurate determinations of the values of quark masses and of the elements of the CKM matrix which are fundamental parameters of the theory and are mandatory inputs to extract a picture for the mass generation mechanism.

Acknowledgements

These lectures have been based, mainly, on results obtained by my colleagues working in the different LEP experiments. I would like to thank, more specifically, members of the LEP heavy flavour working groups who prepared a large fraction of the numbers quoted in this report. Special thanks to F. Parodi and A. Stocchi for our fruitful collaboration. On theoretical aspects I have benefitted from discussions with I.I. Bigi, G. Martinelli and N. Uraltsev. I thank also the organizers of this seminar for the pleasant stay in Sitges.

[6]This by no mean implies that they will not do a very large number of interesting measurements which will improve our knowledge of b-hadrons.

References

[1] ALEPH 2000-068 CONF (CONFerence) 2000-046.

[2] D.E. Groom *et al.*, Eur. Phys. J. **C15** (2000) 1.

[3] P. Roudeau (Orsay, LAL). LAL-97-96, Dec 1997; Lectures given at International School of Physics, 'Enrico Fermi': Heavy Flavor Physics - A Probe of Nature's Grand Design, Varenna, Italy, 8-18 Jul 1997.

[4] DELPHI Collaboration, EPS-HEP99, contributed paper 5.515.

[5] P. Abreu *et al.*, Delphi Collaboration, Zeit. Phys. **C71** (1996) 539.

[6] P. Abreu *et al.*, DELPHI Collaboration, Zeit. Phys. **C74** (1997) 19.

[7] P. Abreu *et al.*, DELPHI Collaboration, Z. Phys. **C76** (1997) 579.

[8] G. Abbiendi *et al.*, OPAL Collaboration, Phys. Lett. **B493** (2000) 266.

[9] P. Abreu *et al.*, DELPHI Collaboration, CERN-EP-2001-002, accepted by Phys. Lett. B.

[10] G. Abbiendi *et al.*, OPAL Collaboration, Phys. Lett. **B482** (2000) 15.

[11] D. Buskulic *et al.*, ALEPH Collaboration, Phys. Lett. **B278** (1992) 209.

[12] P. Abreu *et al.*, DELPHI Collaboration, Zeit. Phys. **C68** (1995) 541.

[13] Combined results on b-hadron production rates, lifetimes, oscillations and semileptonic decays (ALEPH, CDF, DELPHI, L3, OPAL, SLD), SLAC-PUB-8492, CERN-EP-2000-096 and CERN-EP-2001-050.

[14] A.F. Falk and M.E. Peskin, Phys. Rev. **D49** (1994) 3320;
J.G. Körner, Nucl. Phys. Proc. Suppl. **50** (1996) 130.

[15] J. Lee-Franzini *et al.*, CUSB Collaboration, Phys. Rev. Lett. **65** (1990) 2947.

[16] P. Abreu *et al.*, DELPHI Collaboration, Phys. Lett. **B289** (1992) 199.

[17] J. Chay, H. Georgi and B. Grinstein, Phys. Lett. **B247** (1990) 399.

[18] G. Bellini, I.I. Bigi and P.J. Dornan, Phys. Rep. **289** (1997) 1
and references therein.

[19] M. Neubert and C.T. Sachradja, Nucl. Phys. **B483** (1997) 339.

[20] M. Di Pierro and C.T. Sachradja, Nucl. Phys. **B534** (1998) 373.

[21] M. Di Pierro, C.T. Sachradja and C. Michael, (hep-lat/9906031).

[22] M. Beneke *et al.*, Phys. Lett. **B459** (1999) 631, M. Beneke and A. Lenz, (hep-ph/0012222), Talk presented at the UK Phenomenology Workshop on Heavy Flavour and CP violation, 17-22 September 2000, St John's College, Durham, proceedings to appear in J. Phys. G.

[23] D. Becirevic, D. Meloni, A. Retico, V. Gimenez, V. Lubicz and G. Martinelli, Eur. Phys. J. **C18** (2000) 157, (hep-ph/0006135).

[24] M. Acciarri *et al.*, L3 Collaboration, Phys. Lett. **B438** (1998) 417.

[25] P. Abreu *et al.*, DELPHI Collaboration, Eur. Phys. J **C16** (2000) 555.

[26] D. Buskulic *et al.*, ALEPH Collaboration, Phys. Lett. **B377** (1996) 205;
K. Ackerstaff *et al.*, OPAL Collaboration, Phys. Lett. **B426** (1998) 161;
F. Abe *et al.*, CDF Collaboration, Phys. Rev. **D59** (1999) 032004.

[27] R. Barate *et al.*, ALEPH Collaboration, Phys. Lett. **B486** (2000) 286.

[28] F. Abe *et al.*, CDF Collaboration, Phys. Rev. **D57** (1998) 5382.

[29] A.J. Buras, W. Slominski and H. Steger, Nucl. Phys. bf B245 (1984) 369.

[30] H. Albrecht *et al.*, ARGUS Collaboration, Phys. Lett. **B192** (1987) 245.

[31] C. Albajar *et al.*, UA1 Collaboration, Phys. Lett. **B186** (1987) 247, erratum ibid **B197** (1987) 565.

[32] D. Buskulic *et al.*, ALEPH Collaboration, Phys. Lett. **B313** (1993) 498.

[33] H.-G. Moser and A. Roussarie, Nucl. Instrum. Meth. **A384** (1997) 491;

[34] M. Ciuchini, "The CKM-matrix analysis revisited", XXXVI th Rencontres de Moriond, March 10-17, 2001.

[35] G. Brandenburg *et al.*, CLEO Collaboration, CLEO CONF 00-6, contribution at ICHEP2000.

[36] M. Beneke, F. Maltoni and I.Z. Rothstein, Phys. Rev. **D59** (1999) 054003.

[37] P. Abreu *et al.*, DELPHI Collaboration, Phys. Lett. **B426** (1998) 193.

[38] A.S. Chou *et al.*, SLD Collaboration, SLAC-PUB-8686, talk presented at the DPF-2000 meeting, 9-12 Aug. 2000, Ohio State University, Ohio.

[39] C. Greub, P. Liniger, Phys. Lett. **B494** (2000) 237; Phys. Rev. **D63** (2001) 054025;
P. Liniger, (hep-ph/0011093).

[40] A. Kagan, (hep-ph/9806266);
A. Kagan, J. Rathsman, (hep-ph/9701300);
A. Kagan, Phys. Rev **D51** (1995) 6196;
Z. Xiao, C. Li and K. Chao, Phys. Rev. **D62** (2000) 094008.

[41] R. Barate *et al.*, ALEPH Collaboration, Eur. Phys. J. **C4** (1998) 387.

[42] CLEO Collaboration, Phys. Rev. Lett. **80** (1998) 1150.

[43] C. Schwanda, DELPHI Collaboration, DELPHI 2000-105 CONF 404, contributed paper to ICHEP2000.

[44] P. Gagnon, *Semileptonic b branching fractions at LEP*, EPS-HEP99, Tampere (Finland).

[45] B.C. Barish *et al.*, CLEO Collaboration, Phys. Rev. Lett. **76** (1996) 1570.

[46] I.I. Bigi, M. Shifman, N. Uraltsev and A. Vainshtein, Phys. Rev. **D56** (1997) 4017.

[47] A. H. Hoang, Phys. Rev. **D61** (2000) 034005, (hep-ph/9905550).

[48] K. Melnikov, A. Yelkhovsky, Phys. Rev. **D59** (1999) 114009.

[49] M. B. Voloshin, Int. J. of Mod. Phys. **A10** (1995) 2865.

[50] P. Ball and V. Braun, Phys. Rev. **D49** (1994) 2472,
E. Bagan, P. Ball, V. Braun and P. Gosdzinsky, Phys. Lett. **B342** (1995) 362.

[51] I.I. Bigi, M. Shifman, N. Uraltsev and A. Vainshtein, Phys. Rev. **D52** (1995) 196, Int. J. Mod. Phys. **A9** (1994) 2467,
M. Shifman, N. Uraltsev and A. Vainshtein, Phys. Rev. **D51** (1995) 2217.

[52] I.I. Bigi, M. Shifman and N. Uraltsev, Annu. Rev. Nucl. Part. Sci. **47** (1997) 591.

[53] I.I. Bigi, Plenary Talk given at ICHEP2000, (hep-ph/0009021).

[54] M.J. Costa and J. Fuster, DELPHI Collaboration, DELPHI 2000-121 CONF 420.

[55] M. Eidemüller and M. Jamin, QCD-2000, Nucl. Phys. Proc. Suppl. **96** (2001) 404, (hep-ph/0010133).

[56] A. Czarnecki and K. Melnikov, Phys. Rev. Lett. **80** (1998) 3189.

[57] F. Abe *et al.*, CDF Collaboration, Phys. Rev. Lett. **74** (1995) 2626;
S. Abachi *et al.*, D0 Collaboration, Phys. Rev. Lett. **74** (1995) 2632.

[58] I.I. Bigi, M. Shifman and N. Uraltsev, Annu. Rev. Nucl. Part. Sci. **47** (1997) 591.

[59] I. Caprini, L. Lellouch and M. Neubert, Nucl. Phys. **B530** (1998) 153;
C.G. Boyd, B. Grinstein and R.F. Lebed, Phys. Rev. **D56** (1997) 6895.

[60] D. Buskulic *et al.*, ALEPH Collaboration, Phys. Lett. **B395** (1997) 373.

[61] K. Ecklund, CLEO Collaboration, hep-ex/0007052.

[62] LEP Working group on $|V_{cb}|$: http://lepvcb.web.cern.ch/LEPVCB/

[63] V. Morenas, A. Le Yaouanc, L. Oliver, O. Pene and J.C. Raynal, Phys. Rev. **D56** (1997) 5668.

[64] A.K. Leibovich, Z. Ligeti, I.W. Stewart and M. B. Wise, Phys. Rev. **D57** (1998) 308 (hep-ph/9705467) and Phys. Rev. Lett. **78** (1997) 3995 (hep-ph/9703213).

[65] R. Barate *et al.*, ALEPH Collaboration, Eur. Phys. J. **C6** (1999) 555.

[66] P. Abreu *et al.*, DELPHI Collaboration, Phys. Lett. **B478** (2000) 14.

[67] M. Acciarri *et al.*, L3 Collaboration, Phys. Lett. **B436** (1998) 174.

[68] N. Uraltsev *et al.*, Eur. Phys. J. **C4** (1998) 453 and
N. Uraltsev, Int. J. Mod. Phys. **A14** (1999) 4641, (hep-ph/9905520).

[69] A.H. Hoang, Z. Ligeti and A.V. Manohar, Phys. Rev. Lett. **82** (1999) 277;
A.H. Hoang, Z. Ligeti and A.V. Manohar, Phys. Rev. **D59** (1999) 074017.

[70] T.P. Cheng and L.F. Li, "Gauge theory of elementary particle physics", Clarendon Press - Oxford - p. 355-360.

[71] L. Wolfenstein, Phys. Rev. Lett. **51** (1983) 1945.

[72] A.J. Buras, M.E. Lautenbacher and G. Ostermaier, Phys. Rev. **D50** (1994) 3433, (hep-ph/9403384).

[73] M. Ciuchini, G. D'Agostini, E. Franco, V. Lubicz, G. Martinelli, F. Parodi, P. Roudeau and A. Stocchi, (hep-ph/0012308).

[74] M. Beneke, G. Buchalla, M. Neubert and C.T. Sachrajda, hep-ph/0007256.

[75] M. Beneke, G. Buchalla, M. Neubert and C.T. Sachrajda, hep-ph/0104110.